Theoretical Alpha-Decay Rates for the Actinide Region

J. K. POGGENBURG
Isotopes Division, Oak Ridge National Laboratory, Oak Ridge, Tennessee
AND
H. J. MANG
Physik Department, Technische Hochschule München, Munich, Germany
AND
J. O. RASMUSSEN*
Departments of Chemistry and Physics, University of California, Berkeley, California
(Received 9 October 1968)

The theoretical development of the microscopic (shell-model) theory of α decay of deformed nuclei is reviewed, and the detailed formulas applying to even- and odd-mass nuclei are presented. Results are presented from new calculations on ground-rotational-band α-decay patterns for even-even nuclei from atomic numbers 90–106. These calculations represent a refinement over previously published work in that particle-number-conserving variational wave functions were used instead of Bardeen-Cooper-Schrieffer (BCS) wave functions. The new results for even nuclei are not, however, very different from the earlier BCS results. The main contribution of this paper is the tabulation of several hundred theoretical α amplitudes for odd-mass nuclei from elements 92–101. The theoretical intensities derived from these tables are compared with experiment for a representative sampling of α emitters. The main factors governing hindrance for unfavored transitions are discussed in terms of loss of the pairing correlation enhancement and in terms of the Nilsson functions of the odd-nucleon wave function.

I. INTRODUCTION

THE strong-coupling theory of rotational nucleonic structure of deformed nuclei of Bohr[1] appeared in 1952 independently of, but almost simultaneously with, the high-resolution α spectroscopic study[2] of ^{242}Cm, which revealed a nuclear rotational-band structure. Since then there has been the challenge to relate the energies and intensities of the rich actinide α spectra to the theory of deformed nuclei. The classification of final states of α decay into rotational bands proceeded rapidly. The qualitative notion of favored α decay (no change of quantum state of the odd nucleon or nucleons) as being much more rapid than unfavored (change of state) α decay was soon established[3] and served well in the assignment of Nilsson quantum numbers to various bands in odd-mass nuclei. In this early period the problem of penetration of the anisotropic Coulomb barrier was treated by coupled-channel analysis, and the experimental relative intensities of transitions to rotational-band members in even nuclei were used to determine the α wave function on the nuclear surface.[4]

It was not until 1962, ten years after Bohr's original paper, that a quantitative microscopic calculation of the α rates appeared (Paper I),[5] relating rates directly to nucleonic Nilsson wave functions. Paper I presented theoretical calculations of the α-decay intensity patterns to the various rotational states of deformed even-even nuclei. The basic formulation was that of shell-model α-decay-rate theory,[6] in which the α-cluster probability at the nuclear surface was projected from the shell-model product wave function of the constituent nucleons. For the calculations in deformed nuclei Nilsson wave functions were used and configuration mixing was brought in through the pairing-force, (Bardeen-Cooper-Schrieffer) (BCS) superfluidity formalism.[7] The important quadrupole coupling effects in the barrier penetrability were approximated by the Fröman matrix method.[8]

Here we shall present the results of refined new calculations for the rotational intensity patterns, as well as many new properties not calculated before.

First, we have used a larger basis set of Nilsson orbitals above and below the Fermi surface for the actinide nuclei. The new set is 25 proton orbitals by 40 neutron orbitals compared with a 10×10 set in Paper I. Since the theoretical α-decay rates were found so sensitive to details of the pairing-force wave functions, we avoided the ordinary BCS wave functions with their fluctuations in particle number and used exclusively the improved (FBCS) wave functions

* New address: Department of Chemistry, Yale University, New Haven, Conn.

[1] A. Bohr, Kgl. Danske Videnskab. Selskab, Mat.-Fys. Medd. **26**, No. 14 (1952).

[2] F. Asaro, F. K. Reynolds, and I. Perlman, Phys. Rev. **87**, 277 (1952).

[3] J. O. Rasmussen, Arkiv Fysik **7**, 185 (1953); A. Bohr, P. O. Fröman, and B. R. Mottelson, Kgl. Danske Videnskab. Selskab, Mat.-Fys. Medd. **29**, No. 10 (1955).

[4] I. Perlman and J. O. Rasmussen, in *Handbuch der Physik*, edited by S. Flügge (Springer-Verlag, Berlin, 1957), Vol. 42, p. 169.

[5] H. J. Mang and J. O. Rasmussen, Kgl. Danske Videnskab. Selskab, Mat.-Fys. Skrifter **2**, No. 3 (1962) (hereafter referred to as Paper I).

[6] H. J. Mang, Z. Physik **148**, 582 (1957); Phys. Rev. **119**, 1069 (1960).

[7] J. Bardeen, L. N. Cooper, and J. R. Schrieffer, Phys. Rev. **108**, 1175 (1957).

[8] P. O. Fröman, Kgl. Danske Videnskab. Selskab, Mat.-Fys. Skrifter **1**, No. 3 (1957).

TABLE I. Transformed amplitudes $\hat{G}_{00}$ for decay of even-even nuclei to ground.

Neutron No.	G_{00} [a] Th	U	Pu	Cm	Cf	Fm	No	Ku[b]	106
136	3.383	3.201							
138	3.285	3.113	2.841						
140	3.128	2.967	2.716						
142	2.893	2.749	2.522	2.233					
144	2.755	2.623	2.417	2.145					
146		2.589	2.390	2.124	2.038				
148		2.250	2.085	1.859	1.801	1.714	1.703		
150			1.764	1.576	1.539	1.468	1.466	1.536	1.349
152			1.532	1.369	1.338	1.277	1.276	1.336	1.176
154				1.602	1.576	1.509	1.520	1.590	1.425
156					1.816	1.739	1.755	1.835	1.648
158						1.801	1.816	1.899	1.700
160							1.804	1.886	1.681

[a] Tabulated values have been multiplied by 100.

[b] Kurchatovium, $Z=104$.

(strictly conserving particle number) developed[9] and tested[10] earlier. Furthermore, these FBCS wave functions were calculated using an attractive δ-function force between like nucleons in Nilsson orbitals, rather than the usual approximation of a constant G for all pairing-force matrix elements.

We have published preliminary calculations[11] of theoretical α-decay rates for some odd-mass nuclei, and the final calculations for ^{241}Am, which led to a new interpretation[12] of the level structure of ^{237}Np. However, we have not previously published any comprehensive work on odd-A nuclei, and such work constitutes a main contribution of this paper.

II. FORMULAS FOR α AMPLITUDES

A brief outline of the theory and the steps involved in the microscopic calculation of the α amplitudes on the nuclear surface will be presented before the anisotropic barrier-penetration problem is examined.

In our formulation of α decay the α internal wave function χ_α is expressed as a Gaussian-type function of the relative coordinates of the protons and neutrons (see Appendix A for detail). One assumes the time-independent wave functions $\Psi_{I\tau}{}^{M}$ for the daughter nucleus referred to a space-fixed coordinate system, and, correspondingly, $\Phi_{I_i\tau_i}{}^{M_i}$ for the parent. By postulating a space-time region with exponential time dependence, one factors out the time-independent probability amplitude

$$g_{IL\tau}{}^{I_i\tau_i}(R)=\left[\binom{N}{2}\binom{Z}{2}\right]^{1/2}\times\sum_{M}(L\,I\,M\,M_i-M\mid I_i\,M_i)\int\Phi_{I_i}{}^{M_i*}\times Y_L{}^{M}(\Omega)\Psi_I{}^{M_i-M}(\eta)\chi_\alpha(\xi)\,d\xi\,d\eta\,d\Omega,\quad(1)$$

where R is the distance between centers of α particle and daughter nucleus; $\Omega=(\theta,\phi)$ = angular coordinates of the α particle in a space-fixed c.m. system; ξ and η are internal coordinates of α particle and daughter, respectively, including the spin coordinates; I_i, I, and L are the angular momenta of parent, daughter, and α particle relative to daughter, respectively; M_i and M represent the spatial projections of the angular momenta of parent and daughter, respectively; and τ_i and τ represent all other quantum numbers needed to specify the wave functions completely. Angular momentum of the system has been conserved by including the Clebsch-Gordan coefficient and summing over the magnetic quantum number M. The binomial coefficient before the integral arises because the final state (α particle+daughter) is not explicitly antisymmetrized for exchange of nucleons between α particle and daughter. The probability amplitude for the wave function of the parent to contain an α particle and daughter of the specified quantum numbers with centers separated a distance R is designated $g_{IL\tau}{}^{I_i\tau_i}(R)$.

If the Φ and Ψ wave functions accurately represented nucleon probabilities and clustering out to sev-

[9] K. Dietrich, H. J. Mang, and J. H. Pradal, Phys. Rev. **135**, B22 (1964).

[10] H. J. Mang, J. K. Poggenburg, and J. O. Rasmussen, Nucl. Phys. **64**, 353 (1965).

[11] H. J. Mang, Ann. Rev. Nucl. Sci. **14**, 1 (1964).

[12] C. M. Lederer, J. K. Poggenburg, F. Asaro, J. O. Rasmussen, and I. Perlman, Nucl. Phys. **84**, 481 (1966).

TABLE II. Reduced relative amplitudes b_2, for $l=2$ α decay of even-even nuclei.

Neutron No.	Th	U	Pu	Cm	b_2 Cf	Fm	No	Ku	106
136	0.999	0.983							
138	0.986	0.971	0.928						
140	0.981	0.966	0.924						
142	0.986	0.971	0.929	0.895					
144	0.998	0.982	0.939	0.905					
146		0.981	0.938	0.903	0.805				
148		0.934	0.891	0.856	0.759	0.724	0.665		
150			0.840	0.805	0.708	0.673	0.612	0.625	0.451
152			0.831	0.796	0.701	0.665	0.605	0.618	0.444
154				0.731	0.635	0.599	0.535	0.548	0.374
156					0.635	0.597	0.532	0.545	0.366
158						0.620	0.554	0.568	0.385
160							0.579	0.593	0.404

eral nuclear radii, one might simply evaluate the α amplitudes g outside the Coulomb barrier and directly evaluate the implied outgoing α flux. As a practical matter, the shell-model determinantal wave functions, even after improvement by extensive pairing-type configuration mixing, are not expected to reproduce nucleon-nucleon correlations or over-all density for distances much beyond the half-density radius. This unreliability is more acute for the three-dimensional harmonic-oscillator wave functions we use than it would be for nucleonic wave functions evaluated in a realistic finite well.

Thus, as in R-matrix theory of nuclear reactions, we must divide space into two regions by a sphere of radius R_0 somewhere in the region of the nuclear surface. The α amplitudes $g(R_0)$ from Eq. (1) may be evaluated and used as boundary conditions to normalize the irregular Coulomb functions that continue the α amplitudes to large distance and relate them to α-decay intensities. In more sophisticated treatments, even for spherical nuclei, the amplitudes g may serve as boundary conditions for coupled-channel numerical integrations through the barrier.[13] The total decay constant may be expressed in the form

$$\lambda=(1/\hbar)\sum_{IL\tau}P_L(\epsilon)\gamma_{I_i\tau_i IL\tau}{}^2, \tag{2}$$

where $P_L(\epsilon)$ is the penetrability factor for an α particle of energy ϵ and relative angular momentum L. The $\gamma_{I_i\tau_i IL\tau}{}^2$ is the reduced width of R-matrix theory and is related to the g as follows:

$$\gamma_{I_i\tau_i IL\tau}{}^2=(\hbar^2/2M)R_0\,|\,g_{IL\tau}{}^{I_i\tau_i}(R_0)\,|^2, \tag{3}$$

where M is the α reduced mass. It is more convenient to work with the dimensionless amplitude G defined by

$$G(R)=R^{3/2}g(R), \tag{4}$$

and it is in this dimensionless form that we will express α amplitudes. Hereafter, the penetrability factor P_L and the reduced width γ^2 depend on the choice of R_0, but their product will not if R_0 is chosen in a region in which the logarithmic derivative of g and of the irregular external α wave function are the same. This point is discussed by Mang and Rasmussen[5] and by Zeh.[14] The matching of logarithmic derivatives is a condition on the applicability of the theory.

Let us now specialize to discuss spheroidal nuclei with large rotational moments of inertia. The wave functions of the parent and daughter nuclei will be taken according to the strong coupling model of Bohr and Mottelson[1,5]:

$$\Phi_{I,q}{}^{M,K}=[(2I+1)/16\pi^2]^{1/2}\times\{D_{MK}{}^I\chi_K+(-1)^{I-K+q}D_{M-K}{}^I\chi_{-K}\}.$$

The α amplitudes at the "joining surface" are most conveniently taken as an expansion in surface harmonics $Y_{LM}(\theta',\psi')$, the angles θ' and ψ' referring to the body-fixed coordinate system with the nuclear symmetry axis as the polar axis. The "joining surface," which corresponds to the sphere of radius R_0, may be of arbitrary size or eccentricity in the microscopic α-particle theory of spherical nuclei; but we may hope that it will approximately satisfy two conditions: that some linear combination of shell-model Slater-determinant wave functions be reasonably faithful in the

[13] E. A. Rauscher, J. O. Rasmussen, and K. Harada, Nucl. Phys. **A94**, 33 (1967).

[14] H. D. Zeh, Z. Physik **175**, 490 (1963).

TABLE III. Reduced relative amplitudes for $l=4$ α decay of even-even nuclei.

Neutron No.	Th	U	Pu	Cm	b_4 Cf	Fm	No	Ku	106
136	0.524	0.466							
138	0.489	0.430	0.312						
140	0.454	0.396	0.278						
142	0.417	0.359	0.240	0.165					
144	0.363	0.304	0.185	0.109					
146		0.278	0.157	0.081	−0.112				
148		0.225	0.104	0.027	−0.166	−0.191	−0.207		
150			0.066	−0.011	−0.206	−0.230	−0.247	−0.247	−0.324
152			0.062	−0.016	−0.211	−0.235	−0.251	−0.252	−0.327
154				−0.045	−0.241	−0.265	−0.284	−0.284	−0.360
156					−0.209	−0.233	−0.253	−0.254	−0.333
158						−0.188	−0.210	−0.210	−0.298
160							−0.159	−0.159	−0.254

interior region near the surface, and that outside the surface the α wave function be capable of accurate integration to infinity by a coupled-channel barrier-penetrability calculation involving a tractable number of nuclear excited states as channels.

Since we use Nilsson wave functions for nucleonic orbitals inside the surface, we choose the joining surface in the tail region of nuclear density and along a surface on which the Nilsson radial parameter is constant. Such a surface, according to a transformation in the appendix in Nilsson's original work, would be a spheroid of about half the eccentricity of the spheroid on which the nuclear density is at half the central value. It is more straightforward in the derivations which follow to consider the Nilsson coordinates as strictly spherical polar, and we shall return finally to reconsider the approximation involved.

There are now two parts to the problem. First, from the linear combination of products of Nilsson functions of the parent we must project onto the joining sphere a product of an α wave function and a particular daughter-state wave function. Second, we must compute a barrier-penetrability matrix that relates the amplitudes on the surface to α amplitudes at large distance, hence to α-group intensities.

With respect to the first part of the problem, let us consider the oversimplified situation of a deformed nucleus consisting of an inert deformed core plus two protons in Nilsson orbitals Ω_p and $\Omega_{p'}$ (Ω here denoting all quantum numbers N, n_z, Λ, Ω needed to label the orbital completely) and two neutrons in orbitals Ω_N and $\Omega_{N'}$. The daughter nucleus we take as the deformed core with no extra nucleons. By approximating the Nilsson wave functions $\psi_{\Omega_i}(r, \theta', \psi')$ as expansions in three-dimensional isotropic harmonic-oscillator functions, we can perform the transformation from the twelve spatial coordinates of the four nucleons into nine relative coordinates and three c.m. coordinates. The desired α amplitudes $G_{LM}(R)$ are obtained by integrating, as in Eq. (1), over all coordinates except the c.m. radial coordinate R. (There is also a sum over spin coordinates, selecting only singlet couplings of like nucleons.) Let us designate this special G_{LM} amplitude in a notation with superscripts labeling the four Nilsson orbitals:

$$\Gamma_{LM}{}^{\Omega_p\Omega_{p'}\Omega_N\Omega_{N'}} = R^{3/2}\sum_{\text{spin}}\int d\xi_\alpha \int d\cos\theta'\, d\psi' \mathcal{A}(\psi_{\Omega_p}{}^*\psi_{\Omega_{p'}}{}^*) \times \mathcal{A}(\psi_{\Omega_N}{}^*\psi_{\Omega_{N'}}{}^*)\chi_\alpha(\xi_\alpha) Y_L{}^M(\theta'\psi'). \quad (5)$$

The script $\mathcal{A}$ implies antisymmetrization of the wave functions, that is, use of a Slater determinantal wave function. The general expressions for evaluation of Eq. (5) in terms of Nilsson coefficients of the four orbitals are rather complicated and are given in Appendix A of this paper.

From the simplified example of two protons and two neutrons in a potential well we must go on to consider a more realistic nucleus, and to explicitly consider many nucleons outside a core. From the expressions of Eq. (5) or Appendix A for the α amplitude Γ associated with four particular Nilsson orbitals we construct an α projection operator $O_{\alpha LM}$ to accomplish the first part of our task. The operator is most conveniently expressed in second-quantized notation, with $a_{\Omega_p}{}^\dagger$ as creation operator for a proton in state Ω_p and $b_{\Omega_N}{}^\dagger$ that for a neutron in state Ω_N:

$$O_{\alpha LM} = \sum_{\Omega_1\Omega_2\Omega_3\Omega_4} \Gamma_{LM}{}^{\Omega_1\Omega_2\Omega_3\Omega_4}(R) a_{\Omega_1}{}^\dagger a_{\Omega_2}{}^\dagger b_{\Omega_3}{}^\dagger b_{\Omega_4}{}^\dagger. \quad (6)$$

TABLE IV. Reduced relative amplitudes for $l=6$ α decay of even-even nuclei.

Neutron No.	Th	U	Pu	Cm	b_6 Cf	Fm	No	Ku	106
136	−0.038	−0.085							
138	−0.065	−0.111	−0.192						
140	−0.090	−0.135	−0.215						
142	−0.114	−0.159	−0.238	−0.276					
144	−0.137	−0.182	−0.260	−0.297					
146		−0.179	−0.256	−0.292	−0.356				
148		−0.154	−0.226	−0.260	−0.316	−0.303	−0.241		
150			−0.180	−0.212	−0.264	−0.250	−0.186	−0.195	−0.092
152			−0.174	−0.206	−0.259	−0.245	−0.182	−0.191	−0.089
154				−0.111	−0.159	−0.144	−0.077	−0.086	0.020
156					−0.126	−0.111	−0.046	−0.055	0.049
158						−0.087	−0.023	−0.032	0.064
160							0.001	−0.007	0.082

The sum runs over all Nilsson orbitals, and the quantum number Ω_i implies all Nilsson quantum numbers specifying an orbital. The sum is, of course, restricted so that the four nucleon angular-momentum components Ω_i must sum to M, the projection of α angular momentum along the nuclear symmetry axis.

The desired α amplitude G from Eq. (4) for complex nuclear wave functions is obtained by sandwiching the α operator of Eq. (6) between parent wave function (on the left) and daughter wave function (on the right), expressing them in second-quantized form. We consider several cases.

A. Case I: Favored Decay of Even Nuclei

A particular case of interest is decay to the ground rotational band of an even nucleus using BCS wave functions. We write the parent wave function in the usual notation

$$\Phi_i=\prod_{\Omega_p}(U_{\Omega_p}+V_{\Omega_p}a_{\Omega_p}{}^{\dagger}a_{-\Omega_p}{}^{\dagger})\times\prod_{\Omega_N}(U_{\Omega_N}+V_{\Omega_N}b_{\Omega_N}{}^{\dagger}b_{-\Omega_N}{}^{\dagger})\,|\,0\rangle \quad (7)$$

and write similarly for the daughter except with primes on the U and V parameters. Using the anticommutation relations of the operators, it is easy to derive the following:

$$G_{L0}(\text{favored, even})=\langle\Phi_i\,|\,O_{\alpha LM}\,|\,\Phi_f\rangle=\sum_{\Omega_p\Omega_N}\Gamma_{L0}{}^{\Omega_p-\Omega_p\Omega_N-\Omega_N}\times\frac{V_{\Omega_p}U_{\Omega_p}{}'V_{\Omega_N}U_{\Omega_N}{}'}{(U_{\Omega_p}U_{\Omega_p}{}'+V_{\Omega_p}V_{\Omega_p}{}')(U_{\Omega_N}U_{\Omega_N}{}'+V_{\Omega_N}V_{\Omega_N}{}')}\times\prod_{\Omega_p}(U_{\Omega_p}U_{\Omega_p}{}'+V_{\Omega_p}V_{\Omega_p}{}')\prod_{\Omega_N}(U_{\Omega_N}U_{\Omega_N}{}'+V_{\Omega_N}V_{\Omega_N}{}'). \quad (8)$$

It is interesting to note the form of Eq. (8) in the limit of very strong pairing correlation, where the gap parameter Δ is much greater than the average Nilsson level spacing. In this limit the parent and daughter wave functions are the same. With this approximation, Eq. (8) simplifies to

$$G_{L0}\approx\sum_{\Omega_p\Omega_N}\Gamma_{L0}{}^{\Omega_p-\Omega_p\Omega_N-\Omega_N}V_{\Omega_p}U_{\Omega_p}V_{\Omega_N}U_{\Omega_N}. \quad (9)$$

For $L=0$ it turns out that all Γ_{00} coefficients are positive, and if we assume them equal to some average constant value $\Gamma_{00}{}^{\text{av}}$, we get the interesting approximate result

$$G_{00}\approx\Gamma_{00}{}^{\text{av}}\sum_{\Omega_p}U_{\Omega_p}V_{\Omega_p}\sum_{\Omega_N}U_{\Omega_N}V_{\Omega_N};$$

but these sums for the constant-pairing-force approximation are simply equal to the gap parameter Δ divided by the pairing matrix element G.

Thus

$$G_{00}\approx\Gamma_{00}{}^{\text{av}}(\Delta_p/G_p)(\Delta_N/G_N). \quad (10)$$

The pairing force is seen to bring out a large enhancement of the $L=0$ favored decay, since the ratios Δ/G range from 4 to 8 and are measures of the effective number of Nilsson orbitals involved in pairing configuration mixing.

Favored decay of an odd-mass or odd-odd nucleus will have an expression for G_{L0} like Eq. (8), except that the sum will exclude the term for any orbital occupied by an odd nucleon.

B. Case II: Unfavored Decay of Odd-Mass Nuclei

In unfavored decay, by definition the odd nucleon occupies a different Nilsson orbital in parent (K) and daughter (K'). Here the double sum of Eq. (8) be-

TABLE V. Reduced relative amplitudes for $l=8$ α decay of even-even nuclei.

Neutron No.	Th	U	Pu	Cm	b_8 Cf	Fm	No	Ku	106
136	−0.124	−0.140							
138	−0.131	−0.146	−0.159						
140	−0.136	−0.149	−0.160						
142	−0.139	−0.152	−0.160	−0.150					
144	−0.135	−0.145	−0.149	−0.136					
146		−0.127	−0.130	−0.115	−0.045				
148		−0.072	−0.069	−0.052	0.025	0.036	0.054		
150			−0.010	0.009	0.088	0.098	0.113	0.117	0.168
152			0.004	0.022	0.101	0.110	0.124	0.129	0.176
154				0.077	0.156	0.160	0.168	0.175	0.205
156					0.144	0.147	0.152	0.159	0.183
158						0.149	0.154	0.161	0.184
160							0.149	0.155	0.176

comes a single sum:

$$G_{L\,K-K'}=V_{K'}U_{K'}\prod_{\Omega_N\neq KK'}(U_{\Omega_N}U_{\Omega_N}'+V_{\Omega_N}V_{\Omega_N}')\times\prod_{\Omega_p}(U_{\Omega_p}U_{\Omega_p}'+V_{\Omega_p}V_{\Omega_p}')\times\sum_{\Omega_p}[V_{\Omega_p}U_{\Omega_p}'/(U_{\Omega_p}U_{\Omega_p}'+V_{\Omega_p}V_{\Omega_p}')]\times\Gamma_{L\,K-K'}{}^{\Omega_p-\Omega_p\,K-K'},$$

$$G_{L\,K+K'}=V_{K'}U_{K'}\prod_{\Omega_N\neq KK'}(U_{\Omega_N}U_{\Omega_N}'+V_{\Omega_N}V_{\Omega_N}')\times\prod_{\Omega_p}(U_{\Omega_p}U_{\Omega_p}'+V_{\Omega_p}V_{\Omega_p}')\times\sum_{\Omega_p}[V_{\Omega_p}U_{\Omega_p}'/(U_{\Omega_p}U_{\Omega_p}'+V_{\Omega_p}V_{\Omega_p}')]\times(-1)^{q_f+1}\Gamma_{L\,K+K'}{}^{\Omega_p-\Omega_p\,K\,K'},\quad(11)$$

where $(-1)^{q_f}=\pi_f$ is the parity of the daughter nucleus. This phase factor arises because of the symmetrization of the wave function in the strong coupling model of Bohr and Mottelson. These amplitudes for unfavored decay are generally considerably smaller than the favored $L=0$ amplitudes of case I; first, because the coherent sum in one kind of nucleon orbital is lost, and second, because the amplitude $\Gamma_{LM}{}^{\Omega-\Omega\,K-K'}$ for unlike orbitals is usually much smaller than $\Gamma_{L0}{}^{\Omega-\Omega\,\Omega'-\Omega'}$ for time-reversed conjugate orbits.

It should be noted here that the earlier calculations of Paper I were based on BCS wave functions, but the calculations of this paper actually use only the refined particle-conserving projected wave functions denoted FBCS and discussed in Ref. 10. The modified FBCS formulas for α decay corresponding to Eqs. (8) and (11) are similar in appearance and are given by Poggenburg[15] in the appendix of his paper.

[15] J. K. Poggenburg, University of California Radiation Laboratory Report No. UCRL-16187 (unpublished).

III. ANISOTROPIC BARRIER-PENETRATION FORMULAS

Having expressions for the α amplitudes on the spherical "joining surface" of radius R, we must now consider the second part of the problem: the derivation of a barrier-transmission matrix that will relate these amplitudes to outgoing α-wave amplitudes on a sphere at large distance, hence to α intensities. It would be completely inappropriate to use ordinary irregular Coulomb functions to propagate the amplitudes from nuclear surface R to infinity, for the anisotropic barrier through which the α wave must propagate produces a strong coupling between channels involving nuclear rotational states differing in spin by one or two units.

It is convenient to renormalize the barrier-transmission matrix by factoring out penetration factors $P_l(\epsilon)$ calculated as for an undeformed sphere of the same volume. This done, we have the problem of calculating matrices $B_{I_f}{}^{L\,K_i\pm K_f}$ in the following equation for the partial decay constant from nucleus I_iK_i to a state I_fK_f with α orbital angular momentum l:

$$\lambda_{I_f\,K_f l}{}^{I_iK_i}=(1/\hbar)P_l(\epsilon_{I_f})(\hbar^2/2MR_0^2)\times\Big|\sum_L B_{l\,I_f}{}^{L\,K_i-K_f}G_{L\,K_i-K_f}+(-1)^{I_i-L-K_f}B_{l\,I_f}{}^{L\,K_i+K_f}G_{L\,K_i+K_f}\Big|_{R=R_0}{}^2=(1/\hbar)P_l(\epsilon_{I_f})(\hbar^2/2MR_0^2)\,|\,\hat{G}_l\,|^2.\quad(12)$$

In some cases $P_l(\epsilon)$ may be taken simply as the reciprocal of the square of the irregular Coulomb function at the radius R_0; in the numerical work reported here $P_l(\epsilon)$ is evaluated by WKB numerical integration through the entire barrier defined by an optical-model nuclear potential without channel coupling. The specific channel-coupling effects are absorbed into matrices B.

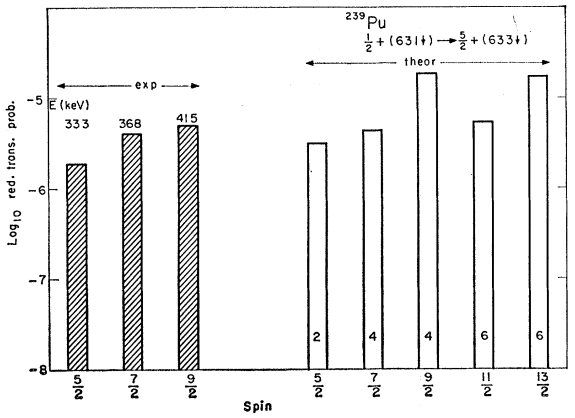

FIG. 1. Comparison of squares of theoretical α amplitudes $|\hat{G}_{LIJ}|^2$ with experimental reduced transition probabilities. The α groups are from ^{239}Pu decay to the $\frac{5}{2}+$ (633) band.

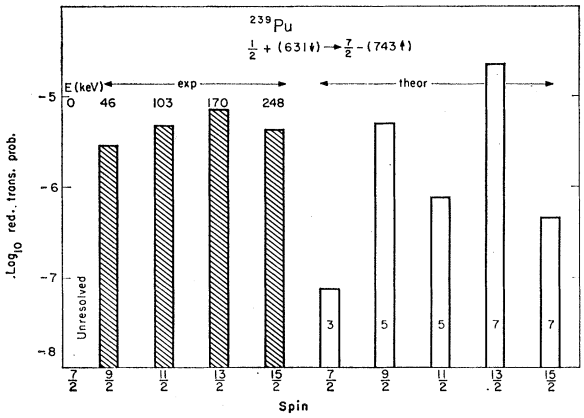

FIG. 3. Comparison of squares of theoretical α amplitudes with experimental reduced transition probabilities in ^{239}Pu α decay to the $\frac{7}{2}-$ (743) band.

The coupled radial Schrödinger equations have been given in greatest generality by Tamura.[16] Outside the range of nuclear forces the coupling is predominantly of electric quadrupole type, involving exchange of two units of angular momentum between nuclear rotation and α orbital motion. Numerical integrations of the coupled equations in spherical polar representation outside the nuclear force region for ^{242}Cm decay[17] showed the barrier-transmission matrix to be somewhat asymmetric, with appreciable first off-diagonal elements. The matrix elements also had small imaginary components, to be associated with Coulomb excitation, an effect of quadrupole coupling outside the barrier in shifting phases of regular and irregular solutions from the normal Coulomb phases.

Numerical integrations in prolate spheroidal coordinates by Rasmussen and Segall[18] and by Pennington and Preston[19] implicitly took into account the stronger coupling setting in at the edge of the attractive nuclear potential well. Referred to spherical polar basis, this coupling in the nuclear surface region is of opposite sense and dominates coupling effects due to the electric quadrupole moment.

The above-mentioned numerical integration studies have been used to test the more convenient Fröman matrix approximation, and for the purpose of the extensive calculations we report here, the Fröman matrix method has been used.

The Fröman matrix carries out the following idealized transformation: Given some arbitrary wave-amplitude function over a surface, usually taken as spheroidal, near the nuclear surface, the function is mapped onto a sphere outside the barrier by multiplying the amplitude at each surface point (θ, ϕ) by the one-dimensional WKB exponential factor along a radial path. The function on the outer surface is renormalized by dividing by the WKB exponential factor for an undistorted sphere enclosing the same volume as the inner surface. The vector composed of the spherical harmonic expansion coefficients of the amplitude on the inner surface, when multiplied from the left by the Fröman matrix, gives the expansion coefficients on the outer sphere. This approximation reproduces the most important effects of the anisotropic barrier, namely that the distribution on the inner surface will be distorted by an enhancement in the region of the thinner barrier (polar regions for a prolate spheroid) in transmission to the outer sphere. For an undeformed nucleus the Fröman matrix becomes a unit matrix.

The treatment of the three-dimensional barrier propagation by one-dimensional radial path integrals is an approximation exact in the limit of vanishing nuclear rotational energy (i.e., infinite moment of inertia) and vanishing kinetic energy of orbital motion [i.e., van-

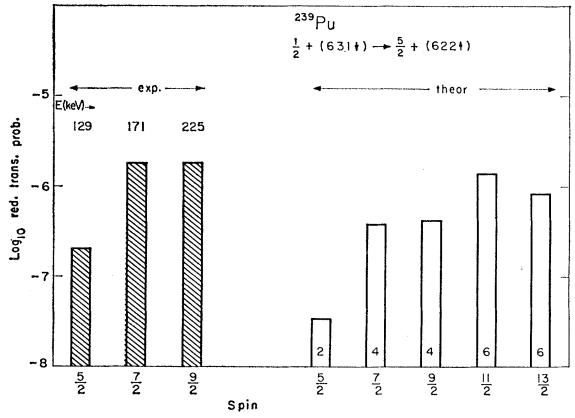

FIG. 2. Comparison of squares of theoretical α amplitudes with experimental reduced transition probabilities in ^{239}Pu α decay to the $\frac{5}{2}+$ (622) band.

[16] T. Tamura, Rev. Mod. Phys. **37**, 679 (1965).
[17] J. O. Rasmussen and E. R. Hansen, Phys. Rev. **109**, 1656 (1958).
[18] J. O. Rasmussen and B. Segall, Phys. Rev. **103**, 1298 (1956).
[19] E. M. Pennington and M. A. Preston, Can. J. Phys. **36**, 944 (1958).

TABLE VI. α amplitudes for odd-proton cases.[a]

Daughter \ Parent	$\frac{5}{2}^+$ [642] ^{237}Np			$\frac{5}{2}^-$ [523] ^{241}Am			$\frac{3}{2}^-$ [521] ^{245}Bk	
$\frac{1}{2}^-$ [530]	0.100(−2)			−0.698(−4)				
	0.205(−2)			−0.747(−4)	0.761(−3)			
	0.264(−2)	0.144(−2)		−0.560(−4)	0.821(−3)			
	0.215(−2)	0.370(−2)		−0.305(−4)	0.112(−2)	0.138(−2)		
	0.132(−2)	0.413(−2)	0.105(−2)	−0.108(−4)	0.484(−3)	0.127(−2)		
	0.489(−3)	0.423(−2)	0.351(−2)	0.448(−3)	0.281(−2)	0.114(−2)		
	0.244(−2)	0.322(−2)	0.285(−3)	−0.729(−4)	−0.899(−3)	−0.903(−3)		
	0.108(−2)	0.416(−2)	0.179(−2)	0.138(−2)	0.265(−2)			
$\frac{5}{2}^+$ [642]	0.213(−1)	0.122(−1)	0.114(−2)	0.664(−3)	0.350(−3)	0.112(−3)	−0.212(−2)	−0.173(−2)
	0.141(−1)	0.308(−2)	−0.161(−3)	0.420(−3)	0.626(−3)	−0.104(−3)	−0.364(−2)	−0.121(−2)
	0.834(−2)	0.456(−2)	−0.568(−3)	0.624(−3)	0.160(−4)	0.714(−3)	−0.341(−2)	−0.654(−3)
	0.423(−2)	−0.111(−2)	−0.188(−3)	0.353(−3)	−0.779(−4)	−0.133(−2)	−0.230(−2)	−0.440(−3)
	0.232(−2)	−0.143(−2)	−0.555(−3)	−0.344(−4)	0.149(−3)	0.112(−2)	−0.141(−2)	0.176(−2)
	−0.123(−2)	−0.981(−3)		−0.270(−4)	−0.130(−2)	−0.206(−2)	0.600(−3)	0.369(−3)
$\frac{5}{2}^-$ [523]	0.337(−3)	0.171(−3)	0.512(−4)	0.170(−1)	0.986(−2)	0.508(−3)	−0.761(−3)	0.160(−2)
	0.213(−3)	0.306(−3)	−0.495(−4)	0.114(−1)	0.137(−2)	−0.349(−3)	−0.878(−3)	−0.134(−2)
	0.305(−3)	0.366(−5)	0.343(−3)	0.674(−2)	0.203(−2)	−0.123(−2)	−0.654(−3)	0.262(−2)
	0.172(−3)	−0.409(−4)	−0.643(−4)	0.188(−2)	−0.242(−2)	−0.355(−3)	−0.958(−3)	0.270(−2)
	−0.203(−4)	0.693(−4)	0.538(−3)	0.103(−2)	−0.310(−2)	−0.105(−2)	0.148(−2)	0.259(−2)
	−0.148(−4)	−0.630(−3)	−0.994(−3)	0.266(−2)	−0.186(−2)		−0.703(−3)	−0.225(−2)
$\frac{3}{2}^-$ [521]				−0.166(−3)	0.192(−3)		0.143(−1)	0.557(−2)
				−0.204(−3)	−0.316(−3)		0.893(−2)	0.323(−3)
				−0.152(−3)	−0.719(−4)	0.432(−3)	0.666(−2)	0.792(−3)
				−0.678(−4)	−0.310(−3)	−0.609(−3)	0.999(−3)	−0.861(−3)
				−0.143(−3)	0.499(−3)	0.414(−3)	0.682(−3)	−0.183(−2)
				−0.905(−4)	−0.397(−3)	−0.510(−3)	−0.214(−2)	−0.351(−3)
				0.151(−3)	0.735(−3)		−0.140(−2)	−0.702(−3)
$\frac{3}{2}^+$ [651]	−0.176(−2)	−0.762(−3)		0.140(−3)	0.393(−4)			
	−0.215(−2)	−0.128(−2)		0.915(−4)	0.786(−4)	−0.882(−4)		
	−0.161(−2)	−0.289(−2)	−0.109(−2)	0.373(−4)	0.908(−4)	−0.261(−4)		
	−0.232(−2)	−0.276(−2)	−0.785(−3)	0.685(−4)	−0.424(−3)	0.187(−3)		
	−0.104(−2)	−0.168(−2)	−0.668(−3)	0.314(−4)	−0.467(−3)	−0.970(−3)		
	−0.187(−2)	−0.156(−2)		−0.348(−3)	−0.177(−3)	0.562(−3)		
				−0.162(−3)	−0.110(−2)	−0.122(−2)		

TABLE VI (*Continued*)

Daughter \ Parent	$\frac{7}{2}^+$ [633] ^{253}Es				$\frac{7}{2}^-$ [514] ^{257}Md			
$\frac{5}{2}^+$ [642]	0.143(−2)	0.437(−3)	0.229(−3)		0.994(−5)	−0.118(−3)		
	0.140(−2)	0.922(−3)	−0.225(−3)		0.812(−5)	−0.261(−3)	−0.102(−2)	
	0.884(−3)	0.120(−2)	0.546(−4)	0.236(−3)	0.513(−5)	−0.354(−3)	0.111(−2)	
	0.345(−3)	0.108(−2)	−0.216(−3)	−0.632(−3)	0.245(−5)	−0.348(−3)	−0.141(−2)	−0.921(−3)
	0.693(−3)	−0.113(−3)	−0.117(−3)		0.774(−6)	−0.255(−3)	0.556(−3)	0.166(−2)
	0.280(−3)	−0.156(−3)	−0.104(−2)		−0.138(−3)	−0.866(−3)	−0.158(−2)	
					−0.482(−4)	0.326(−4)	0.177(−2)	
$\frac{3}{2}^-$ [521]	−0.148(−2)	−0.378(−3)						
	−0.210(−2)	−0.532(−3)						
	−0.200(−2)	−0.153(−2)	−0.415(−4)					
	−0.141(−2)	−0.176(−2)	0.192(−3)					
	−0.734(−3)	−0.189(−2)	0.496(−4)	0.198(−3)				
	−0.248(−3)	−0.135(−2)	0.299(−3)	0.375(−3)				
	−0.765(−3)	0.149(−3)	0.876(−3)					
$\frac{7}{2}^+$ [633]	0.125(−1)	0.525(−2)	−0.893(−3)	−0.976(−4)	−0.222(−3)	−0.144(−3)	0.627(−4)	−0.470(−4)
	0.501(−2)	−0.175(−2)	−0.365(−3)	0.438(−4)	−0.119(−3)	−0.204(−3)	0.167(−3)	0.612(−4)
	0.254(−2)	−0.206(−2)	−0.775(−3)	0.201(−3)	−0.170(−3)	0.266(−3)	0.443(−4)	−0.636(−3)
	−0.160(−2)	−0.111(−2)	0.522(−3)		−0.828(−4)	0.287(−3)	0.145(−3)	0.688(−3)
	−0.760(−3)	−0.114(−2)	0.925(−3)		0.214(−3)	0.169(−3)	−0.813(−3)	
$\frac{7}{2}^-$[514]					0.137(−1)	0.591(−2)	−0.859(−3)	−0.109(−3)
					0.564(−2)	−0.168(−2)	−0.409(−3)	0.422(−4)
					0.286(−2)	−0.199(−2)	−0.868(−3)	0.194(−3)
					−0.154(−2)	−0.125(−2)	0.503(−3)	
					−0.731(−3)	−0.127(−2)	0.892(−3)	

[a] Amplitude entries have the power of 10 in parentheses. The successive rows refer to successive spin states in the daughter rotational band starting with the band-head value ($=K$). Successive columns refer to successive allowed L values, starting in the leftmost column with the minimum L value, the next column being $L_{min}+2$, the next $L_{min}+4$, etc.

TABLE VII. α amplitude

Parent / Daughter	$\frac{5}{2}^+$ [633] ^{233}U				$\frac{7}{2}^-$ [743] ^{235}U			
	0.225(−3)	0.508(−3)						
	0.276(−3)	−0.341(−3)						
	0.206(−3)	0.431(−3)	0.103(−2)					
$\frac{3}{2}^+$ [631]	0.920(−4)	−0.886(−5)	−0.149(−2)					
	0.187(−3)	0.116(−2)	0.112(−2)					
	0.334(−4)	−0.998(−3)	−0.193(−2)					
	0.332(−3)	0.169(−2)						
	0.207(−1)	0.116(−1)	0.165(−2)		−0.638(−3)	−0.848(−3)	−0.121(−3)	
	0.134(−1)	0.445(−2)	−0.181(−4)		−0.347(−3)	−0.125(−2)	−0.367(−3)	−0.397(−3)
	0.792(−2)	0.658(−2)	−0.640(−4)		−0.123(−3)	−0.117(−2)	−0.648(−3)	0.522(−3)
$\frac{5}{2}^+$ [633]	0.611(−2)	−0.125(−3)	−0.226(−3)		−0.751(−3)	−0.792(−3)	−0.251(−3)	−0.537(−3)
	0.335(−2)	−0.161(−3)	−0.668(−3)		−0.301(−3)	−0.703(−3)	0.486(−3)	0.108(−2)
	−0.138(−3)	−0.118(−2)			−0.447(−3)	0.928(−4)	−0.499(−3)	
	−0.212(−3)	−0.282(−3)	−0.401(−4)		0.203(−1)	0.132(−1)	0.245(−2)	−0.533(−4)
	−0.425(−3)	−0.132(−3)	0.156(−3)		0.126(−1)	0.479(−2)	−0.199(−3)	−0.448(−4)
$\frac{7}{2}^-$ [743]	−0.312(−3)	−0.231(−3)	−0.114(−3)		0.636(−2)	0.565(−2)	−0.423(−3)	−0.205(−3)
	−0.250(−3)	0.145(−3)	0.268(−3)		0.439(−2)	−0.607(−3)	−0.534(−3)	
	−0.156(−3)	0.277(−4)	−0.213(−3)		0.208(−2)	−0.621(−3)	−0.946(−3)	
	−0.307(−3)							
	−0.328(−3)	−0.336(−3)						
	−0.246(−3)	−0.632(−3)						
$\frac{1}{2}^+$ [631]	−0.134(−3)	−0.875(−3)	−0.347(−3)					
	−0.474(−4)	−0.725(−3)	−0.600(−3)					
	−0.476(−3)	−0.932(−3)	−0.158(−3)					
	−0.179(−3)	−0.748(−3)	−0.244(−3)					
	−0.549(−3)	−0.434(−3)						
$\frac{5}{2}^+$ [622]								
		^{238}U				^{235}U		
	−0.921(−3)	−0.433(−3)	0.303(−4)		0.148(−2)	0.640(−3)	−0.120(−3)	
	−0.582(−3)	−0.775(−3)	−0.373(−4)		0.145(−2)	0.135(−2)	0.286(−3)	
$\frac{5}{2}^-$ [752]	−0.773(−3)	−0.120(−4)	0.536(−3)		0.915(−3)	0.175(−2)	0.311(−3)	−0.207(−3)
	−0.437(−3)	−0.448(−4)	−0.191(−3)		0.357(−3)	0.159(−2)	0.706(−3)	0.141(−3)
	−0.298(−4)	0.102(−2)	0.817(−3)		0.102(−2)	0.740(−3)	−0.431(−3)	
	−0.184(−4)	0.475(−3)	−0.606(−3)		0.410(−3)	0.683(−3)	−0.141(−3)	
		$\frac{7}{2}^+$ [624] ^{245}Cm				$\frac{9}{2}^-$ [734] ^{249}Cf		
	−0.281(−3)	−0.188(−4)	−0.579(−3)		0.114(−2)	0.225(−3)	−0.858(−4)	
	−0.275(−3)	−0.397(−4)	0.510(−3)		0.132(−2)	0.520(−3)	−0.163(−4)	
$\frac{5}{2}^+$ [622]	−0.174(−3)	−0.515(−4)	−0.260(−3)	−0.840(−3)	0.108(−2)	0.769(−3)	−0.256(−3)	0.252(−4)
	−0.678(−4)	−0.467(−4)	0.334(−3)	0.113(−2)	0.676(−3)	0.843(−3)	−0.348(−3)	−0.216(−3)
	−0.298(−4)	−0.413(−4)	−0.104(−2)		0.316(−3)	0.715(−3)	−0.538(−3)	−0.219(−3)
	−0.121(−4)	0.178(−3)	0.834(−3)		0.976(−4)	0.472(−3)	−0.544(−3)	−0.601(−3)
	0.126(−1)	0.809(−2)	0.649(−3)	−0.157(−3)	0.363(−3)	0.454(−3)	−0.650(−5)	−0.191(−4)
	0.772(−2)	0.127(−2)	−0.587(−3)	−0.414(−4)	0.173(−3)	0.563(−3)	−0.145(−4)	−0.777(−4)
$\frac{7}{2}^+$ [624]	0.391(−2)	0.150(−2)	−0.125(−2)	−0.190(−3)	0.548(−4)	0.458(−3)	−0.207(−4)	−0.184(−3)
	0.117(−2)	−0.179(−2)	−0.493(−3)		0.261(−3)	−0.214(−4)	−0.306(−3)	0.282(−3)
	0.553(−3)	−0.183(−2)	−0.874(−3)		0.943(−4)	−0.165(−4)	−0.383(−3)	−0.299(−3)
					0.900(−2)	0.499(−2)	−0.190(−3)	−0.215(−3)
$\frac{9}{2}^-$ [743]					0.415(−2)	−0.310(−3)	−0.586(−3)	0.107(−5)
					0.187(−2)	−0.314(−3)	−0.990(−3)	0.292(−5)
					0.216(−3)	−0.119(−2)	0.554(−5)	
$\frac{7}{2}^+$ [613]								
$\frac{1}{2}^+$ [620]								

0.335(−3)
−0.382(−3)

for odd-neutron cases.

$\frac{1}{2}^+$ [631] ^{239}Pu				$\frac{5}{2}^+$ [622] ^{243}Cm			
−0.174(−2)				−0.142(−2)	−0.287(−3)		
0.114(−2)				−0.174(−2)	−0.367(−3)		
−0.450(−2)				−0.130(−2)	−0.945(−3)	0.495(−5)	
0.325(−2)				−0.581(−3)	−0.909(−3)	0.694(−3)	
−0.450(−2)				−0.741(−3)	0.535(−3)	0.119(−3)	
0.318(−2)				−0.327(−3)	0.939(−3)	0.777(−3)	
−0.177(−2)				0.527(−3)	0.718(−3)		
−0.178(−2)				−0.688(−3)	−0.177(−3)	0.818(−4)	
−0.209(−2)				−0.205(−3)	0.221(−3)	−0.651(−3)	
−0.431(−2)				−0.121(−3)	0.326(−3)	0.740(−3)	
−0.233(−2)				0.303(−3)	−0.371(−3)	−0.105(−2)	
−0.418(−2)				0.166(−3)	0.443(−3)	0.128(−2)	
−0.869(−3)				0.165(−4)	−0.132(−2)		
0.273(−3)				0.915(−3)	0.954(−3)	0.208(−4)	
0.226(−2)				0.144(−2)	0.682(−4)	−0.251(−3)	
0.882(−3)				0.106(−2)	0.120(−3)	−0.124(−4)	
0.481(−2)				0.129(−3)	−0.760(−3)	−0.123(−3)	
0.673(−3)				0.811(−4)	−0.881(−3)	−0.132(−3)	
0.145(−1)				0.294(−3)			
0.791(−2)				0.315(−3)	0.113(−2)		
0.969(−2)				0.236(−3)	−0.100(−2)		
0.150(−2)				0.128(−3)	0.176(−2)	0.133(−2)	
0.168(−2)				0.454(−4)	−0.514(−3)	−0.205(−2)	
−0.230(−2)				0.729(−3)	0.252(−2)	0.651(−3)	
−0.248(−2)				−0.617(−4)	−0.173(−2)	−0.137(−2)	
−0.116(−2)				0.116(−2)	0.136(−2)		
0.184(−3)				0.157(−1)	0.931(−2)	0.501(−3)	
−0.612(−3)				0.108(−1)	0.135(−2)	−0.309(−3)	
0.643(−3)				0.636(−2)	0.200(−2)	−0.109(−2)	
−0.118(−2)				0.186(−2)	−0.214(−2)	−0.284(−3)	
0.908(−3)				0.102(−2)	−0.274(−2)	−0.839(−3)	
−0.818(−3)				−0.236(−2)	−0.148(−2)		

$\frac{7}{2}^+$ [613] ^{255}Fm				$\frac{9}{2}^+$ [615] ^{257}Fm			
0.124(−1)	0.562(−2)	−0.950(−3)	−0.136(−3)	0.158(−3)	−0.245(−4)	−0.633(−5)	0.582(−3)
0.536(−2)	−0.186(−2)	−0.509(−3)	0.497(−4)	0.134(−3)	−0.414(−4)	−0.187(−4)	−0.457(−3)
0.272(−2)	−0.220(−2)	−0.108(−2)	0.228(−3)	0.746(−4)	−0.453(−4)	−0.342(−4)	0.334(−3)
−0.171(−2)	−0.155(−2)	0.592(−3)		0.262(−4)	−0.358(−4)	−0.449(−4)	−0.192(−3)
−0.809(−3)	−0.159(−2)	0.105(−3)		−0.204(−4)	−0.448(−4)	0.145(−3)	
−0.604(−3)							
−0.768(−3)							
−0.154(−2)	−0.386(−3)						
−0.119(−2)	−0.340(−3)						
−0.113(−2)	−0.113(−2)	0.108(−3)					
−0.582(−3)	−0.678(−3)	0.439(−3)					
−0.308(−3)	−0.978(−3)	0.437(−3)					
−0.835(−4)	−0.416(−3)	0.732(−3)					

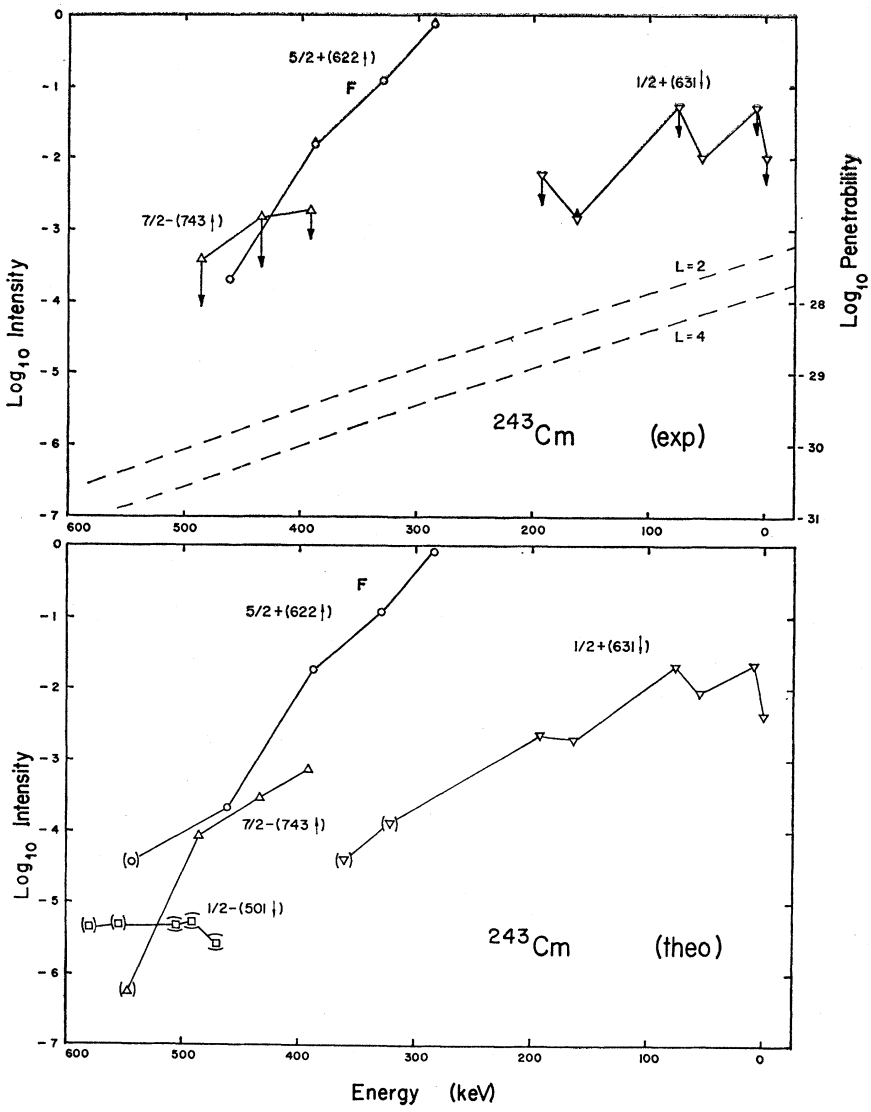

FIG. 4. Plot of relative α intensities of ^{243}Cm as a function of excitation energy of the final state; the intrinsic bands are labeled by asymptotic quantum numbers and the rotational members are connected by a line; the arrows on the experimental plot (top) indicate the position of the corresponding theoretical point of the graph below; the broken lines give the value of the penetrability factor for some representative l waves as a function of the excitation energy. Ordinary parentheses on points in the lower diagram indicate predictions for states not yet observed experimentally. Points in horizontal parentheses have been seen in β decay but not in α decay. The Nilsson state of the parent may be read near the letter F designating the favored band.

ishing of the "centrifugal energy" term $(\hbar^2/2mr^2)l(l+1)$ in the coupled radial equations]. Of course, these energy terms with their substantial effects on barrier penetrability are not ignored in the over-all expressions based on the Fröman matrix; rather, they are approximately factored out into the penetration factor $P(\epsilon_{I_f})$ in Eq. (12). As some studies have indicated, this approximation should be good in general, the exception being α groups which are weak relative to a group populating an adjacent rotational-band member.

The Fröman matrix for pure quadrupole shape deformation has elements given by

$$k_{lL}{}^m = \int Y_l{}^{m*} \exp[BP_2(\cos\theta)]Y_L{}^m d\Omega, \qquad (13)$$

where the argument B is the difference of WKB path integrals at $\theta=\cos^{-1}\sqrt{\frac{2}{3}}$ and $\theta=0$. That is,

$$B=\frac{\sqrt{2m}}{\hbar}\int_R^{R_t}\{[V(r,0)-E]^{1/2} -[V(r,\cos^{-1}\sqrt{\tfrac{2}{3}})-E]\}dr,$$

with R_t the outer classical turning point where the integral becomes a complex number. The $m=0$ matrix elements of Eq. (13) were tabulated for a range of arguments by Fröman, but we needed the $m\neq 0$ matrices; for convenience these matrix elements are tabulated in Appendix B up to $m=9$ for a single argument: $B=0.9$.

For favored decay of a spin-zero nucleus the B matrices of Eq. (12) are equal to the Fröman matrix. That is,

$$B_{lI_f}{}^{L0}=\delta_{lI_f}k_{lL}{}^0. \qquad (14)$$

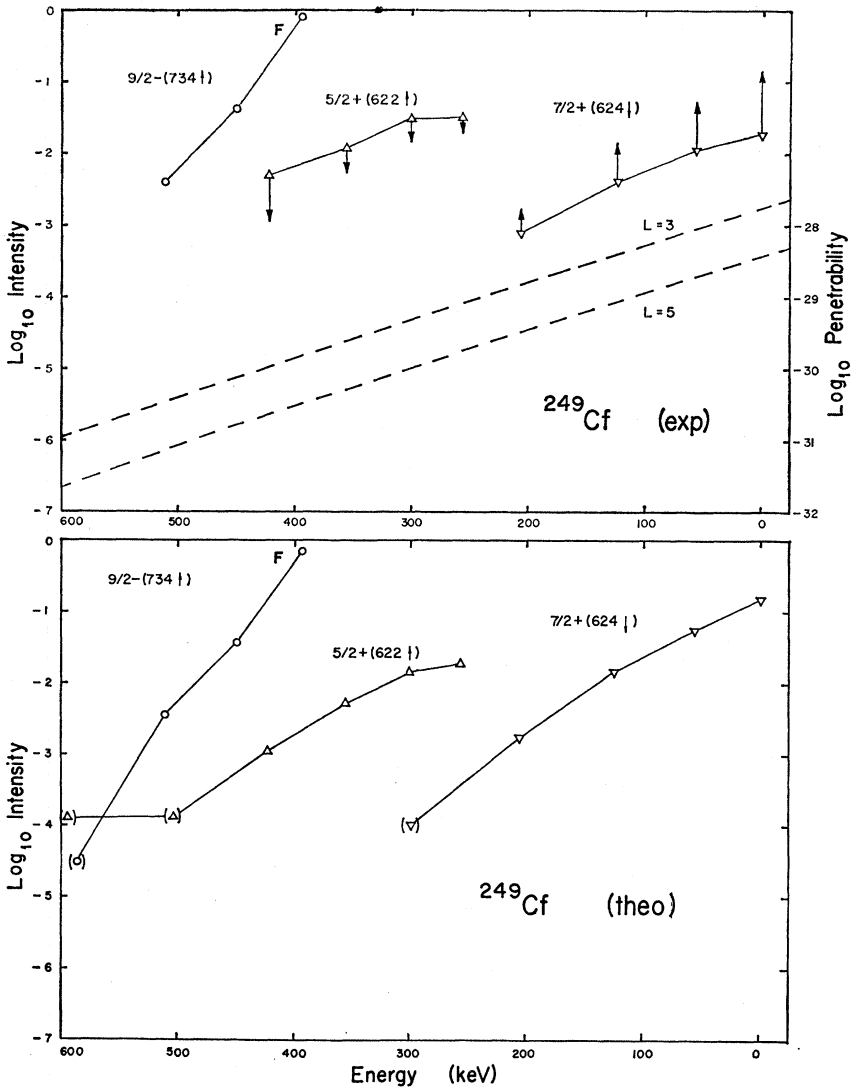

FIG. 5. Plot of relative α intensities of ^{249}Cf as a function of excitation energy of the final state; the notation is similar to that for Fig. 4.

For nonzero spin of the parent, the B matrices are more complicated, since the Fröman k matrix extends the α wave function onto a sphere at large distance but in the body-fixed coordinate system with indices I_i and l and with their respective projections K_i and m on the nuclear symmetry axis. It is necessary, finally, to transform to the representation with definite final-state spin I_f replacing index m. Bohr, Fröman, and Mottelson[3] first considered this transformation and the general intensity relations implied. The transformation coefficients are Clebsch-Gordan coefficients, so that we have the following expression for the B-matrix elements of Eq. (12):

$$B_{l\,I_f}{}^{L\,K_i-K_f} = (-)^{l+K_i-K_f}(I_i\,l\,K_i\,K_f-K_i\,|\,I_f\,K_f)k_L{}^{K_i-K_f}, \quad (15a)$$

$$B_{l\,I_f}{}^{L\,K_i+K_f} = (-)^{l+K_i+K_f}(I_i\,l\,-K_i\,K_f+K_i\,|\,I_f\,K_f)k_L{}^{K_i+K_f}. \quad (15b)$$

We note again that the barrier-propagation treatment of Eqs. (12), (13), and (15) is approximate except in the limits of infinite moment-of-inertia or zero deformation. Numerical integration of coupled-channel equations provides a better treatment. We have referred to such work for even nuclei.[17] We do not know of any coupled-channel numerical studies testing the Fröman matrix method for nonzero-spin parents.

IV. NUMERICAL CALCULATIONS

The results presented in this paper have extended the earlier calculations of Paper I to include 25 proton and 40 neutron orbitals (instead of the earlier 10×10 set) outside an arbitrary core which does not participate in the formation. Thus, for even-even calculations, each G_{L0} involves the sum over a thousand Γ coefficients. In addition, the results of calculations for a large number of odd-mass nuclides are presented. Another refinement in the procedure is the use of particle-

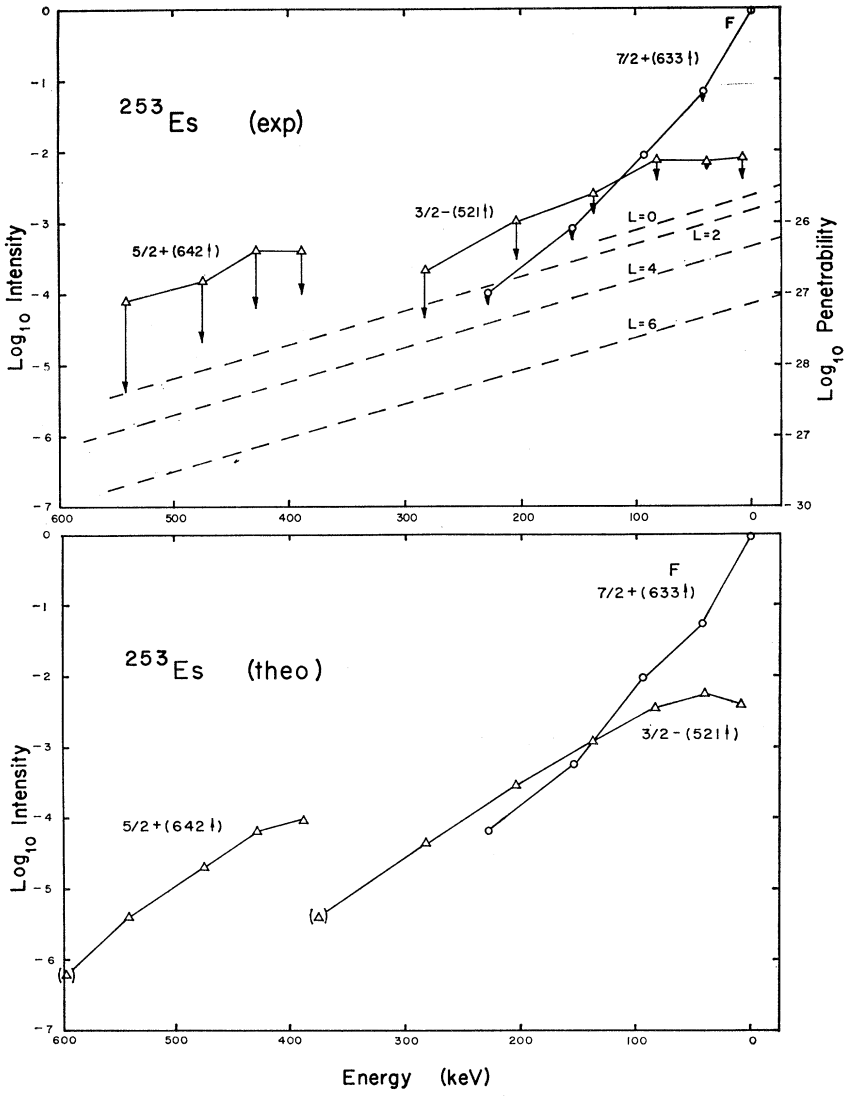

FIG. 6. Plot of relative α intensities of ^{253}Es as a function of excitation energy of the final state; the notation is similar to that for Fig. 4. The serious disagreement with theory for the uppermost band is attributed to strong Coriolis mixing with the favored band.

number-conserving FBCS occupation probabilities. The sample odd-mass calculations given in Mang's Table III[11] included the same orbitals, but the ordinary BCS calculations were used for the occupation probabilities.

The calculations are performed using the $|\,l\Lambda\Omega\rangle$ representation of Nilsson,[20,21] with Ω the total angular-momentum projection on the nuclear symmetry axis, and the expansion coefficients $a_{l\Lambda}$ of an orbital of negative projection taken with the same sign as for positive Ω. The orbital states are labeled with the usual asymptotic quantum numbers of Nilsson, N, n_z, Λ, and Ω, with the projection of the particle spin angular-momentum Σ given by $\Sigma+\Lambda=\Omega$. The Γ_{LM} coefficients depend upon the choice of size parameters α, β, and R_0, but they can be expanded in terms of $C_\rho{}^L$ coefficients which depend only on the orbital wave functions. β is the α-particle size parameter which is fixed at 0.47 fm^{-2} to correspond to the measured rms charge radius of 1.6 fm for an α particle. The parameter α expresses the nuclear size and is given by $m\omega_0/\hbar$, for which Nilsson has given the relation $\hbar\omega_0\approx 41A^{-1/3}$ MeV. For $A=238$ the parameter α has the value 0.1597 fm^{-2}. In the special limit that the oscillator constant α for the nucleon wave functions is the same as the oscillator constant β for the internal motion in the α cluster, the evaluation of amplitudes is especially easy. Early work of Mang[6] and some work of Sandulescu[22] employed this simplifying approximation. There is a close relation here to successive transformations by Moshinsky brackets to relative and c.m. representations. The joining radius R_0 is fixed somewhat arbitrarily at 8.25 fm for these calculations, so as to be beyond the last radial maxi-

[20] S. G. Nilsson, Kgl. Danske Videnskab. Selskab, Mat.-Fys. Medd. **29**, No. 16 (1955).

[21] B. R. Mottelson and S. G. Nilsson, Kgl. Danske Videnskab. Selskab, Mat.-Fys. Skrifter **1**, No. 8 (1959).

[22] A. Sandulescu and M. Stihi, Nucl. Phys. **37**, 344 (1962).

mum in the shell-model wave functions. We previously observed (Paper I)[5] that the G amplitudes are not very sensitive to variations of α and R_0 which maintain αR_0^2 constant. Therefore, instead of decreasing α and increasing R_0 with A, we have kept α and R_0 fixed at these values for all the actinides.

The equations used for calculating Γ have been given before (Paper I), but they are repeated in Appendix A for convenience. The computer programs are written mostly in FORTRAN IV for the IBM 7094 with some machine-language modifications. The Clebsch-Gordan coefficients are computed by a machine-language subroutine obtained from Los Alamos Laboratory. The steps in the calculation of the α-formation factor are (a) calculation of the $C_\rho{}^L$ coefficients, which are stored on tape, (b) calculation of the FBCS occupation probabilities, which are punched out on cards, and (c) calculation of the probability amplitudes G_{LM} at the nuclear surface using the output from steps (a) and (b). The G_{LM} are punched on cards that are used as input for the program multiplying by the penetration matrices of Eq. (12). One set of $C_\rho{}^L$ coefficients applies to all even-even transitions and also to all favored transitions of odd-mass nuclei. The $C_\rho{}^L$ coefficients for hindered decays must be calculated uniquely for the orbitals involved. The L expansion is terminated at $L=8$ for even series and at $L=9$ for odd series. The same matrix elements are used throughout, for we have not tried to vary deformation as far as Nilsson coefficients are concerned. The Nilsson deformation parameter of about $\eta=5$ would be most appropriate as an average for actinide nuclei, but the $C_\rho{}^L$ coefficients are calculated with the Nilsson coefficients from Ref. 21 at deformation parameter $\eta=4$, since we wished to avoid difficulties of interpolation. The Nilsson orbital energies used are those appropriate to $\eta=5$, but the energies have been somewhat shifted from Nilsson's values to match better the experimental energies of the various bands. The FBCS wave functions and orbital energies were thoroughly discussed in a previous publication[10]; one may judge from that paper how well the experimental odd-even mass differences and spectra were matched and what defects might reflect themselves in the α amplitudes calculated here.

We have carried out these calculations for ground band decay of even-even nuclei from elements 90–106 and from neutron numbers 136–160. We have not treated decay to "vibrational" or "two-quasiparticle" bands, but we refer the reader to the work of Sandulescu *et al.*[23] for a microscopic treatment of such decay. We have carried out our α theoretical calculations for odd-mass nuclei from ^{229}Th to ^{257}Md; only decay to pure one-quasiparticle Nilsson bands is considered. Thus, modifications for Coriolis admixing and three-quasiparticle ("phonon") components are yet to be made, but the α amplitudes given in this paper may be a useful starting point for studies of Coriolis-mixing modifications.

We have not treated any odd-odd nuclei, although our results may be used for neighboring odd-mass nuclei as a guide to expected hindrance factors. In Ref. 15, calculations were carried through and tabulated as theoretical partial-decay-rate constants according to Eq. (12). For calculations on undiscovered nuclei or α groups, it was not practical to calculate a barrier-penetrability factor $P(\epsilon_{I_f})$, since this factor is too sensitive to decay energy for predicted decay energies to be used. Thus, for these unknown cases, the α amplitudes [within absolute value signs in Eq. (12)] and their squares were given without inclusion of the penetration factor.

For this paper we wish to present just the α amplitudes that depend only on the Nilsson wave functions and pairing-force strength. The α amplitudes are independent of the myriad experimental α-decay energies of varying uncertainty, of state assignments, of questions about the proper optical-model potential for barrier calculations, and of questions on correcting for mismatch of logarithmic derivatives of internal and external solutions.

One should consult Ref. 15 for a more complete tabulation of predicted intensities with penetrability factors taken as the WKB exponential through a barrier defined by a nuclear potential

$$V(r)=-V_r\{1+\exp[(r-R_0)/a]\}^{-1}, \qquad (16)$$

with $V_r=74$ MeV, $a=0.565$ fm, and $R_0=(1.17A^{1/3}+1.6)$ fm.

The α amplitudes presented here can be squared and multiplied by the factor of 8 to normalize to the laboratory system[24] and by any desired penetrability factors to give relative decay rates. We found that our absolute theoretical decay rates using the above potential and Eq. (12) are smaller than experiment by about an order of magnitude. Thus, in Ref. 15, one arbitrary normalization factor was applied for the several hundred theoretical rate constants, the factor being determined to make exact agreement for the ground decay of ^{238}Pu. It is difficult to say whether this discrepancy in absolute rate theory is due to the use of harmonic-oscillator nucleon wave functions, to the neglect of all nucleon-nucleon correlations except those represented by pairing within one to two major shells, or to the use of an incorrect potential for the barrier. Whatever the cause of the absolute rate discrepancy, the correction is sufficiently uniform that the relative rates are in remarkably good agreement with experiment in most cases. Recent work[25] suggests, however, that the α-

[23] A. Sandulescu, Nucl. Phys. **48**, 345 (1963); Phys. Letters **19**, 404 (1965); A. Sandulescu and O. Dumitrescu, *ibid.* 24B, 212 (1967); Nucl. Phys. **A100**, 456 (1967).

[24] J. Eichler and H. J. Mang, Z. Physik **183**, 321 (1965).

[25] L. McFadden and G. R. Satchler, Nucl. Phys. **84**, 177 (1966); W. J. Thompson, G. E. Crawford, and R. H. Davies, *ibid.* **A98**, 228 (1967); Gy. Bencze and A. Sandulescu, Phys. Letters **22**, 473 (1966); Gy. Bencze, *ibid.* **23**, 713 (1966); L. Scherk and E. W. Vogt, Can. J. Phys. **46**, 1119 (1968).

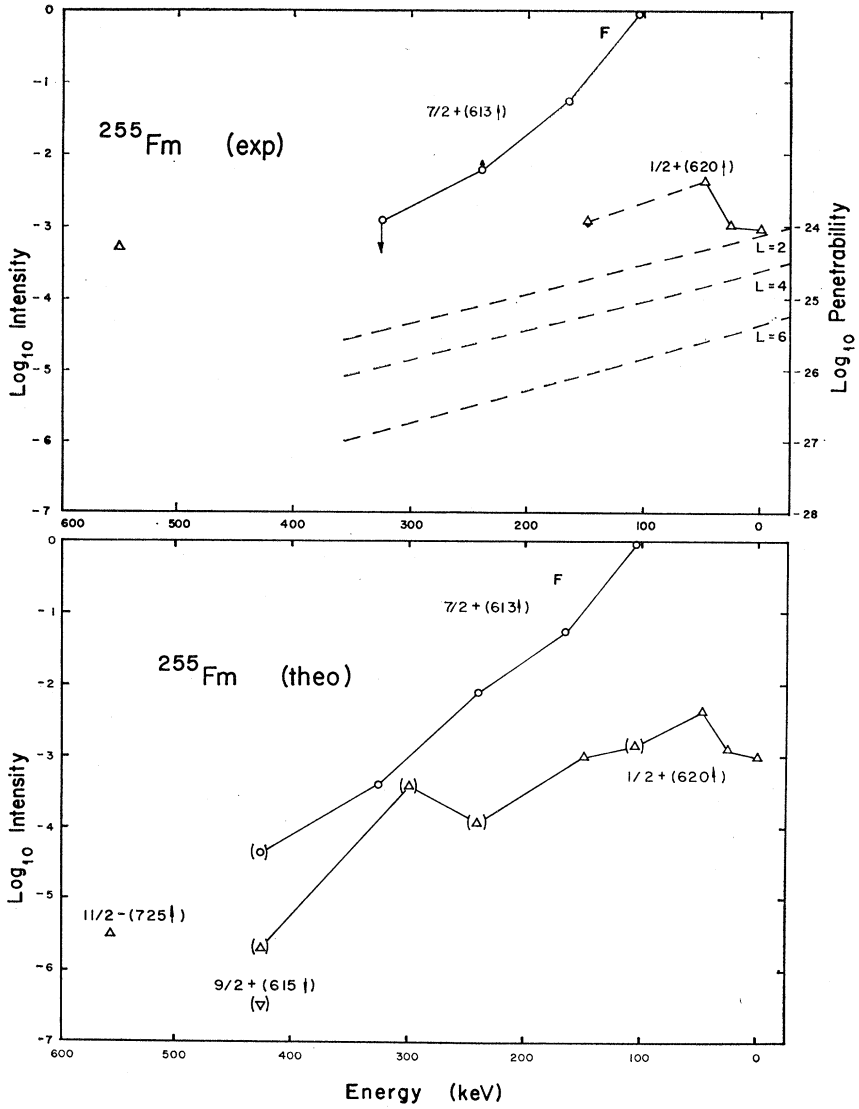

FIG. 7. Plot of relative α intensities of ^{255}Fm as a function of excitation energy of the final state; the notation is similar to that for Fig. 4. The theoretical calculations for the $11/2-$ and $\frac{9}{2}+$ bands were speculative. The unusually intense group at 0.55-MeV excitation (hindrance factor ~ 70) is probably the band head of a $\frac{5}{2}+$ band, with α decay enhanced by Coriolis coupling as in the topmost band shown in Fig. 6.

nucleus potential [Eq. (16)] and the WKB approximation we used are subject to corrections that could account for the entire discrepancy.

To a slight extent the numerical α amplitudes tabulated here are dependent on the barrier-penetrability assumptions. The argument B for the Fröman matrices was determined empirically to give the best over-all relative intensity patterns for the rotational bands of the even-even nuclei. Though B is expected to vary with changing deformation, we chose the one fixed value $B=0.9$ for all nuclei in order to reduce the number of arbitrary parameters. This value is rather close to that given by the following formula of Paper I, based on more fundamental considerations:

$$B=6.1\delta-0.045Q_0, \qquad (17)$$

where δ is Nilsson's surface deformation parameter, and Q_0 is the intrinsic quadrupole moment in barns. The reasoning used to derive the above formula considered the G_L vectors as specifying the α wave function on the spheroidal Nilsson-coordinate surface of about half the eccentricity of the isopotential surface. Nilsson's introduction of this special deformed coordinate system was to compensate for his explicit exclusion of $N=\pm 2$ admixtures in the wave functions. Earlier in this paper we indicated that the α amplitude formulas here are strictly applicable only to the highly symmetrical spherical-polar coordinate system. Our use of a value of B smaller than that of Fröman's formula is due to the need to compensate for neglected $N=\pm 2$ components in the Nilsson wave functions, and also due to the fact that our G vector specifies a distribution on a spherical surface whereas Fröman's initial distribution is on the spheroidal surface of the inner wall of the barrier.

We explored calculations on even-even α decay with

a more general Fröman matrix, including effects of $P_4(\cos\theta)$ distortions of the nuclear surface. We concluded that our theory was not sufficiently accurate to derive such β_4 distortions from experimental even-even intensities. Once there are better independent determinations of β_4 distortions of actinides, similar to the α scattering experiments of Hendrie *et al.*[26] in the rare earths, these effects can easily be included in the Fröman matrix, by making the exponent in Eq. (13) BP_2+DP_4, where D is the coefficient analogous to B.

V. NUMERICAL RESULTS AND COMPARISON WITH EXPERIMENT

First we consider the results of the new calculations for the even-even nuclei. Table I lists the amplitudes $\hat{G}_{00}$ for ground decay. The symbol $\hat{G}_{00}$ represents the amplitude after multiplication by the Fröman matrix, as defined in Eq. (12):

$$\hat{G}_{l0}=\sum_L k_{lL}G_{L0}. \tag{18}$$

A gradual decrease is observed in the α amplitudes in going from lightest to heaviest nuclei, with a minimum for $N=152$. This variation reflects mainly the decrease in pairing correlation due to increasing Nilsson orbital spacing.

Tables II–V give amplitude ratios of G_{L0} for $L=2$, 4, 6, and 8, respectively, relative to the G_{00} values of Table I.

Table II shows that decay to the first excited 2+ state should gradually become more hindered for the heaviest element (106) by over a factor of 6 compared with that for thorium.

Table III shows decay to the 4+ state nearly vanishing for the heavy Cm isotopes, then increasing for the heavier elements. The fact that the high $l=4$ hindrance region coincides with experiment is largely due to our fixing the argument ($B=0.9$) of all Fröman matrices so as to reproduce the region at which maximum $l=4$ hindrance occurs.

The $l=6$ α decay is predicted (Table IV) not to show the striking variation of the $l=4$ over the region of known nuclei. A very high $l=6$ hindrance is predicted in the lightest and in the heaviest nuclei calculated.

It is not clear whether the present theory, without $\Delta N=\pm 2$ mixing in Nilsson functions, can be reliable for $l=8$. The results of Table V are thus to be regarded with skepticism.

The major contribution of this paper is contained in Tables VI and VII, tabulations for odd-mass nuclei of the theoretical α amplitudes $\hat{G}_l$. Many rotational states of many combinations of Nilsson bands are included. To obtain theoretical decay constants, one need only square the amplitudes, multiply by penetration factors appropriate to that l value, and sum the contribution from various l values to a given final state. To obtain absolute rate constants of practical value, one must determine a normalizing factor, perhaps demanding rate agreement for a particular nucleus using a barrier penetrability based on some nuclear potential. If one uses the Woods-Saxon potential of Eq. (16) and normalizes to the ground-state decay of ^{238}Pu, as Poggenburg[15] has done, then the normalizing factor is 6.0×10^{22} sec^{-1}. For α angular-correlation predictions one need only correct the $\hat{G}_l$ values to a given final state by appropriate centrifugal barrier-penetrability corrections; one then has the desired amplitude ratios in the standard phase convention.

From Tables I, VI, and VII we can also extract ratios comparable to the often-used "hindrance factor." For example, for the $l=0$ favored decay of ^{239}Pu we read from Table VII the amplitude 0.014; from Table I the amplitudes for neighboring ^{238}Pu (2.417×10^{-2}) and ^{240}Pu (2.390×10^{-2}) give the average 0.024). Thus the hindrance factor is $(0.024/0.014)^2$. For other α groups consisting of a single l value ($l\neq0$), the theoretical reduced hindrance factor above is to be multiplied by the appropriate barrier factor.[27] For groups with mixed l values the connection to the conventional hindrance factor will require l sums over amplitudes squared times centrifugal factors.

We shall make only a brief comparison with experiment here. For a comparison of experiment and theory one should consult Figs. 4 and 5 of Ref. 11. The main difference between the values listed in Tables II–V and those listed in Ref. 11 is the method of calculation. In the earlier work[11] ordinary BCS wave functions were used, whereas here the particle-number-conserving FBCS wave functions are used. Also, we use $B=0.9$ [Eq. (13)] for all nuclei, whereas in the earlier work the value of B was calculated for each nucleus individually from the formula $B=6.1\delta-0.045Q_0$ given in Paper I. Despite these differences there is not much difference between our new results for even nuclei and those plotted in Ref. 11. The over-all agreement is quite good. The $l=2$ group relative to $l=0$ is underestimated for the lightest nuclei; perhaps the up-sloping Nilsson orbitals from the major shell below contribute too strongly to lower the $l=2$ amplitudes. We have used somewhat too large deformation, and the up-sloping orbitals may be too high in Nilsson's calculation.

In a few favored decay cases the mixture of l values and relative phases has been directly tested by angular-correlation experiments. In most cases the decay group tested is the $\Delta I=0$ favored group.[28] All the experiments

[26] D. L. Hendrie, N. K. Glendenning, B. G. Harvey, O. N. Jarvis, H. H. Duhm, J. Saudinos, and J. Mahoney, Phys. Letters **26B**, 127 (1968).

[27] J. O. Rasmussen, Phys. Rev. **113**, 1593 (1959).

[28] V. E. Krohn, T. B. Novey, and S. Raboy, Phys. Rev. **105**, 234 (1951); K. Siegbahn and F. Asaro, Phys. Letters **2**, 323 (1962).

on the $\Delta I=0$ transitions confirm the theoretical prediction that $l=0$ and $l=2$ amplitudes have the same sign. The limited experimental information bearing on the $l=4$ groups indicates[29] that the phase of $l=2$ and $l=4$ is the same in ^{233}U and opposite in ^{253}Es, in agreement with the theory as given in Tables VII and VI, respectively. No angular-distribution experiments have yet tested l-mixture predictions for hindered decay; inspection of Tables VI and VII shows that considerable admixture usually occurs and that l values other than the minimum may dominate. There have been indirect analyses[30] of l mixtures through analyses of intensity patterns, and these analyses generally agree with our theoretical predictions.

For α emission to or from spin-$\frac{1}{2}$ states, only a single L value is permitted, and comparisons of our theoretical values with experimental intensities are especially simple. For example, for the spin-$\frac{1}{2}$ isotope ^{239}Pu we show in Figs. 1–3 the theoretical results for three final bands as the squares of α amplitudes $\hat{G}_L{}^2$, denoted "reduced transition probability." The experimental values are the partial decay constants λ_{I_f} (in sec^{-1}) divided by the WKB penetrability factor for that l value and divided by the factor 6.02×10^{22} that normalizes the theory to the ^{238}Pu rate. Figures 1 and 2 give the decay patterns to the two $\frac{5}{2}+$ Nilsson bands expected (they are ground bands in ^{233}U and ^{243}Cm, respectively). Theoretically and experimentally, the decay patterns are very different. The decay to the $\frac{5}{2}+$ (633) band is less hindered, and the intensity to the band head is only slightly weaker than those to higher states. The decay to the $\frac{5}{2}+$ (622) band, on the other hand, is more retarded by an order of magnitude, and the decay to the band head is especially suppressed, relative to decay to the higher states. Even though the theory considerably overestimates the retardation of decay to the $\frac{5}{2}+$ (622) band, the qualitative differences are such that the state assignments could be clearly made from α-decay behavior.[11] This assignment of states was later confirmed[31] by the "signatures" from (d, p) and (d, t) reaction studies leading to ^{235}U.

The decay to the ground band (Fig. 3) agrees in over-all hindrance, but shows serious disagreement in the signature. Perhaps Coriolis mixing, probably large in the $\frac{7}{2}-$ (743) state, is responsible for the disagreement.

Another instance in which the theoretical results of this paper proved of great value in assigning states to a decay scheme is the α decay of ^{241}Am. The arguments leading to the assignment of the $\frac{1}{2}-$ (530) band in ^{237}Np have been given by Lederer *et al.*[12]

When a mixture of l values occurs in each α group, it is not so easy to compare theory and experiment as in Figs. 1–3. Therefore in our remaining sample comparisons the fraction of α decay to a group is plotted versus the excitation energy of the final state.[32] The open symbols in Fig. 4 give experimental intensities in ^{243}Cm decay, and the arrowheads mark the corresponding theoretical values. The odd-even staggering pattern, a striking feature of decay to the ground band, is reproduced semiquantitatively. The theory adequately gives the relative intensity signature to the $\frac{7}{2}-$ (743) band, but the theoretical prediction is too low overall by a factor of about 3. Penetrability factors for $l=2$ and 4 are plotted on the right-hand scale to facilitate estimates of hindrance factors.

Figure 5 gives the comparison for ^{249}Cf. Signatures are correctly matched, but the theory overestimates the ground band by factors of 2 to 9 and underestimates the middle band by slightly lower factors.

Figure 6 gives the comparison for ^{253}Es decay. A serious underestimate of the theory is seen for the $\frac{5}{2}+$ (642) band, but this error is clearly a consequence of the strong Coriolis mixing between this band and the favored ground band. These orbitals, being mainly of the high j-value $i_{13/2}$ character, have especially large Coriolis matrix elements. Figure 7 is a similar plot for ^{255}Fm.

One can judge from the foregoing figures the sort of uncertainties to be expected in comparing experiment and theory. For practical purposes of estimating hindrance factors, the details of which penetrability formulas to use are unimportant. The older vertical potential barrier expressions or graphical plots may be used instead of our numerical integration values, which are based on diffuse optical potentials.

VI. SELECTION RULES AND ANALOGIES TO ELECTROMAGNETIC TRANSITION

An old analysis of α hindrance factors by Prior[33] showed the highest hindrances to be associated with $|\Delta\Sigma|=1$ transitions, that is, transitions in which there is a change in relative orientation (parallel or antiparallel) of intrinsic spin and total particle angular momentum on the nuclear Z axis. A study of Table VI sheds light on this matter. For $\Delta\Sigma=0$ the minimum allowed L values (near $|K_i-K_f|$) have not too small amplitudes G. For $|\Delta\Sigma|=1$ the minimum L values may have quite small amplitudes, with only those L values exceeding K_i+K_f becoming large. To the extent that Σ is a good quantum number, one or the other of the two terms in Eq. (12) dominates, since

[29] See discussion in J. O. Rasmussen, in *Alpha, Beta and Gamma Spectroscopy*, edited by Kai Siegbahn (North-Holland Publishing Co., Amsterdam, 1965), Vol. I, p. 742.

[30] F. A. Asaro, S. G. Thompson, F. S. Stephens, and I. Perlman, in *Proceedings of the International Conference on Nuclear Structure, Kingston, Canada, 1960*, edited by D. A. Bromley and E. W. Vogt (The University of Toronto Press, Toronto, Canada, 1960), p. 581.

[31] J. R. Erskine and R. R. Chasman (private communication).

[32] In Figs. 4–6, for comparison, the normalization of theory to ^{238}Pu is replaced by a normalization to the total α-decay rate of the isotope in question, but the difference in normalization is not large.

[33] O. Prior, Arkiv Fysik **16**, 15 (1959).

TABLE VIII. α and "electric multipole" amplitude comparison.

Orbitals	L	M	$G_{E\lambda}$ [Eq. (19)]	G_{LM} (α theory)[a] ^{243}Cm	^{241}Pu	^{239}Pu	^{233}U
$\frac{5}{2}^+$ (622) and $\frac{1}{2}^+$ (631)	2	2	0.0108	0.049	0.053	0.018	
	4	2	0.0304	0.055	0.058	0.020	
	6	2	0.0346	0.011	0.014	0.005	
	8	2	0.0124	0.023	0.023	0.008	
	4	3	0.159	0.172	0.0183	0.061	
	6	3	0.188	0.281	0.302	0.101	
	8	3	0.0498	0.125	0.145	0.048	
$\frac{5}{2}^+$ (622) and $\frac{7}{2}^-$ (743)	1	1	0.016	0.055			
	3	1	0.226	0.146			
	5	1	0.011	0.006			
	7	1	0.124	0.114			
	9	1	0.010	0.030			
	7	6	0.081	0.032			
	9	6	0.029	0.007			
$\frac{1}{2}^+$ (631) and $\frac{5}{2}^+$ (633)	2	2	0.291			0.132	0.040
	4	2	0.308			0.302	0.089
	6	2	0.192			0.271	0.085
	8	2	0.0050			0.045	0.021
	4	3	0.0073			0.013	0.004
	6	3	0.0130			0.026	0.008
	8	3	0.0182			0.015	0.005

[a] Tabulated values have been multiplied by 100.

the like nucleons in the α particle are in a singlet spin state.

We can see the operation of the Σ selection rule more directly by examining the α amplitudes G_{LM} in the body-fixed system, before multiplication by the Fröman matrices. The rightmost columns of Table VIII list the magnitudes $|G_{LM}|$ for a few odd-neutron cases. Note for the first combination of states, where $|\Delta\Sigma|=1$, that the $M=2$ amplitudes are all small relative to the $M=3$ amplitudes. For the second and third combination of states, the Σ selection rule should favor the lower of the two M values, and this is indeed the case.

We note that the relative amplitudes do not change much for different nuclei for a given combination of initial and final states. That is, the two Nilsson functions of the odd nucleon may dominate the calculation.

It would be desirable to find an approximate method for calculating these amplitudes and to find out which aspects are predominant in determining the amplitudes. The "electric transition rule" has been discussed in an earlier review article, and it may be stated as follows: Determine which electric transition multipolarities would be strong or weak between the single-particle states of the odd nucleon in parent and daughter; the strong and weak L values for α decay will generally correspond to the strong and weak electric 2^L-pole transitions.

In order to adapt this rule quantitatively for deformed nuclei, we have taken Nilsson's equation [(35b) in Ref. 21] for a 2^λ-pole transition, replacing radial matrix elements by unity. The angular integrals are similar for electric and α amplitudes, but the α amplitudes depend only on the surface value of the wave function. This procedure gives the following very simple expression:

$$G_{E\lambda}=\sum_{l'l}\left(\frac{2l+1}{2l'+1}\right)^{1/2}(l\,\lambda\,0\,0\,|\,l'\,0)\times\sum_{\Lambda'\Lambda\Sigma'\Sigma}\delta_{\Sigma'\Sigma}a_{l'\Lambda'}a_{l\Lambda}(l\,\lambda\,\Lambda\,K'-K\,|\,l'\,\Lambda'),\quad(19)$$

where the $a_{l\Lambda}$ are normalized Nilsson coefficients. The column headed $|G_{E\lambda}|$ (electric) in Table VIII gives the result of calculations with Eq. (19) and the

TABLE IX. Fröman matrices.

$m=0$, even L

l \ L	0	2	4	6	8
0	1.0906	0.4814	0.0847	0.0097	0.0008
2	0.4814	1.4707	0.4700	0.0778	0.0087
4	0.0847	0.4700	1.4168	0.4546	0.0755
6	0.0097	0.0778	0.4546	1.4069	0.4509
8	0.0008	0.0087	0.0755	0.4509	1.4035

$m=0$, odd L

	1	3	5	7	9
1	1.5211	0.4967	0.0821	0.0091	0.0008
3	0.4967	1.4319	0.4591	0.0762	0.0085
5	0.0821	0.4591	1.4103	0.4523	0.0751
7	0.0091	0.0762	0.4523	1.4049	0.4501
9	0.0008	0.0085	0.0751	0.4501	1.4026

$m=1$, even L

	2	4	6	8
2	1.1960	0.3841	0.0637	0.0071
4	0.3841	1.3480	0.4256	0.0700
6	0.0637	0.4256	1.3760	0.4361
8	0.0071	0.0700	0.4361	1.3858

$m=1$, odd L

	1	3	5	7	9
1	0.8753	0.2999	0.0517	0.0059	0.0005
3	0.2999	1.3074	0.4132	0.0680	0.0075
5	0.0517	0.4132	1.3662	0.4322	0.0711
7	0.0059	0.0680	0.4322	1.3819	0.4386
9	0.0005	0.0075	0.0711	0.4386	1.3885

$m=2$, even L

	2	4	6	8
2	0.7951	0.2113	0.0336	0.0037
4	0.2113	1.1722	0.3477	0.0552
6	0.0336	0.3477	1.2887	0.3937
8	0.0037	0.0552	0.3937	1.3344

$m=2$, odd L

	3	5	7	9
3	1.0391	0.2995	0.0474	0.0051
5	0.2995	1.2455	0.3759	0.0601
7	0.0474	0.3759	1.3161	0.4056
9	0.0051	0.0601	0.4056	1.3473

$m=3$, even L

l \ L	4	6	8
4	0.9488	0.2417	0.0358
6	0.2417	1.1597	0.3299
8	0.0358	0.3299	1.2543

$m=3$, odd L

	3	5	7	9
3	0.7545	0.1611	0.0233	0.0024
5	0.1611	1.0764	0.2944	0.0445
7	0.0233	0.2944	1.2155	0.3546
9	0.0024	0.0445	0.3546	1.2821

$m=4$, even L

	4	6	8
4	0.7302	0.1295	0.0170
6	0.1295	1.0076	0.2529
8	0.0170	0.2529	1.1525

$m=4$, odd L

	5	7	9
5	0.8908	0.2011	0.0278
7	0.2011	1.0915	0.2909
9	0.0278	0.2909	1.1977

$m=5$, even L

	6	8
6	0.8506	0.1714
8	0.1714	1.0374

$m=5$, odd L

	5	7	9
5	0.7141	0.1079	0.0129
7	0.1079	0.9564	0.2205
9	0.0129	0.2205	1.0996

$m=6$, even L

l \ L	6	8
6	0.7028	0.0923
8	0.0923	0.9172

$m=6$, odd L

l \ L	7	9
7	0.8212	0.1490
9	0.1490	0.9940

$m=7$, even L

$k_{88}^{7}=0.7988$

$m=7$, odd L

	7	9
7	0.6943	0.0805
9	0.0805	0.8862

$m=8$, even L

$k_{88}^{8}=0.6878$

$m=8$, odd L

$k_{99}^{8}=0.7812$

$m=9$, odd L

$k_{99}^{9}=0.6826$

same Nilsson coefficients ($\eta=4$) as were used in the sophisticated α amplitude calculations. We note a strong qualitative correlation between results of the two calculations. To obtain the approximate formula [Eq. (19)] from the α amplitude expression (5), one must first assume a point α particle and then assume a wave function of the even nucleon which is constant in angle. The first assumption systematically overemphasizes high L values, but the second may tend to suppress high L values. Thus the simple approximate formula may owe its relative success to a compensation of errors. At any rate, there seems to be a semiquantitative validity to the analogy between the electric transition and hindered α decay. Hence one might also seek evidence for the operation of selection rules in the other asymptotic quantum numbers. In analogy with electric multipole transitions, we might suppose that $L=1$ amplitudes will never be large between low-lying states, since these transitions always violate selection rules in either the spherical or the large deformation limits. Indeed, in none of the cases that we have calculated is there a large $L=1$ amplitude.

VII. CONCLUSION

We have now extensively tested on deformed nuclei the microscopic theory of α decay, in which the α amplitudes at the nuclear surface are projected from the nucleon wave functions in the Nilsson model with pairing-force configuration mixing. The results have given a deeper understanding of rotational-band population signatures and of the widely varying hindrance factors for unfavored decay, in which the Nilsson state of an odd nucleon changes between parent and daughter. We understand that the smooth trends of absolute reduced rates and of rotational-band signatures for favored decay are a consequence of pairing-force mixing, which, in a completely coherent manner, enhances the $L=0$ group by 3 orders of magnitude $[\sim(\Delta_p^2/G_p^2)(\Delta_n^2/G_n^2)]$ and which produces a signature by averaging over the nearest Nilsson orbitals ($\Delta/G\approx 5$–7) about the Fermi energy.

The hindrance of unfavored decay is understood to arise from two principal factors. First, the coherent sum of amplitudes over several Nilsson orbitals is lost for the type of nucleon undergoing a change of state, and this loss is reflected in a lowered rate factor of about $(\Delta/G)^2$. Second, additional hindrance may arise from mismatching of the initial- and final-state Nilsson orbitals, of which the Σ selection rule discussed in Sec. VI is a clear example. The rotational-band signature for hindered decay is largely determined by just the two Nilsson orbitals of the odd nucleon, and the associated α amplitudes bear close analogy to the electric transition matrix elements between the two odd states.

Three questions remain for brief consideration here: What further work in α theory and experiment is needed? What simplifications of these complicated calculations are justified? What may be the consequences in areas of physics outside of α decay?

First, there is need for a systematic comparison of experimental α-decay signatures and angular momentum mixtures with the predictions of Table VI. In some cases it will clearly be important to include Coriolis mixing between bands. It may be valuable to treat the barrier-penetration problem by full coupled-channel numerical integration rather than by the Fröman matrix approximation. It is worthwhile to investigate effects of higher-order (P_4) deformation in the nuclear surface, both through effects on the Nilsson functions and on the barrier-penetration matrix. The effects of three-quasiparticle components (or phonon admixtures) added to one-quasiparticle components may be important, particularly for states at excitations comparable to the gap energy 2Δ. Further attention to the fundamentals of the theory is desirable with regard to the arbitrary choice of the nuclear radius, the problem of harmonic-oscillator wave functions, and a better treatment of the one-body aspects of the problem.

Second, there are two limits that result in simplified theoretical expressions: the point-α limit (δ-function limit) and the limit of α size equal to the nuclear size. The former approximation is probably the more realistic one, though it is known to systematically overestimate amplitudes of higher L values. There is no promising way to avoid the use of numerical coefficients of the Nilsson wave-function type, for there are no obvious representations (cylindrical coordinates, square wells) that are appreciably more diagonal for realistic deformed nuclei. It may be useful to compute tables of Legendre expansion coefficients (separately for neutron and proton) for pair-averaged wave functions on the nuclear surface, for these coefficients would vary smoothly with nucleon number. These tables could be used in conjunction with Fröman matrices to calculate favored decay and in conjunction with the electric-transition equation (19) to calculate hindered-decay properties.

Finally, we expect that the results of this paper have important implications for multinucleon transfer reactions of deformed nuclei, particularly when at least one particle is so strongly absorbed that the reaction is a surface reaction. In the simplest case of nucleon pair transfer, such as (t, p), (p, t), $(^3\mathrm{He}, n)$, $(n, ^3\mathrm{He})$, $(^{12}\mathrm{C}, ^{14}\mathrm{C})$, etc., we expect the pairing enhancement for favored transitions, in which there is no change of state of unpaired nucleons. We expect the rotational-band signatures for favored transitions to reflect the angular zones of the Nilsson wave functions near the Fermi energy. Unfavored transitions with nucleon-state changes will be weaker by hindrance factors comparable to those in α decay, and the rotational-band signatures will be, as in α decay, dominated by initial and final surface wave functions of the odd nucleon. The nu-

clear reaction field should provide great opportunities for further extension of the sensitive probing of nucleon-nucleon correlations provided by the α-decay process.

ACKNOWLEDGMENTS

This work is largely based on the doctoral thesis research of one of us (J. K. P.) during the period when all authors worked at the University of California Lawrence Radiation Laboratory, Berkeley, Calif., under support of the U.S. Atomic Energy Commission. The effective cooperation of the Mathematics and Computing Division in the use of the IBM-7094 is gratefully acknowledged. During the period of writing and analysis we have received support from the Oak Ridge National Laboratory, operated by Union Carbide Corporation under contract to the U.S. Atomic Energy Commission (J. K. P.), from the Technische Hochschule Munich (H. J. M.), and from the University of California and the USAEC [Contract No. AT 11-1 (34)]; also the National Science Foundation (Theoretical Physics Summer Institute at the University of Wisconsin, Summer, 1967) (J. O. R.).

APPENDIX A: DETAILED FORMULAS FOR α-DECAY MATRIX ELEMENTS

The equations used for the calculation of the Γ coefficients have been given before as Eqs. (II.8)–(II.11) in Paper I. They are repeated here without derivation for convenience, with the shorthand notation for angular momentum $[L]=(2L+1)^{1/2}$. The labels 1 and 2 refer to protons, and 3 and 4 to neutrons.

We assume the internal wave function of the α particle to be

$$\chi_\alpha=\chi_0^0(12)\chi_0^0(34)\,(2\beta^{3/2}/\tfrac{1}{2}!4\pi)^{3/2}\times\exp[-\tfrac{1}{2}\beta(\xi_1^2+\xi_2^2+\xi_3^2)],$$

with χ_0^0 the singlet spin functions and ξ_i relative coordinates:

$$\xi_1=\tfrac{1}{2}\sqrt{2}\,|\,\mathbf{r}_1-\mathbf{r}_2\,|,\qquad \xi_2=\tfrac{1}{2}\sqrt{2}\,|\,\mathbf{r}_3-\mathbf{r}_4\,|,$$
$$\xi_3=\tfrac{1}{2}\,|\,\mathbf{r}_1+\mathbf{r}_2-\mathbf{r}_3-\mathbf{r}_4\,|.$$

The size parameter $\beta=0.47$ F^{-2} gives an rms charge radius for the α in agreement with electron scattering data and our calculations.

We assume the Nilsson wave functions of the following form so that the coefficients $A_{l\Lambda}$ are in Nilsson's convention and may be taken directly from his tables with normalization:

$$|\,Nl\Lambda(\Sigma)\Omega\rangle=\sum_{\Omega-1/2\le l\le N}R_{Nl}(r)\left[A_{l\Omega-1/2}\times Y_l^{\Omega-1/2}(\theta,\phi)\begin{pmatrix}1\\0\end{pmatrix}+A_{l\Omega+1/2}Y_l^{\Omega+1/2}(\theta,\phi)\begin{pmatrix}0\\1\end{pmatrix}\right],$$

where the Y_l^m functions are the usual spherical harmonics, and the spin vectors

$$\begin{pmatrix}1\\0\end{pmatrix}\quad\text{or}\quad\begin{pmatrix}0\\1\end{pmatrix}$$

refer to spin projection in the positive or negative direction, respectively, along the nuclear symmetry axis. The radial functions [Eq. (A1)] are best expressed in terms of associated Laguerre functions, although Nilsson's phase convention that the radial functions are positive in the limit of large radius introduces a phase factor in the Laguerre functions:

$$R_{Nl}(r)=(-)^n\left[\frac{2n!\alpha^{3/2}}{(n+l+\frac{1}{2})!}\right]^{1/2}(\alpha r^2)^{l/2}\times L_n^{l+1/2}(\alpha r^2)\exp(-\tfrac{1}{2}\alpha r^2),\quad\text{(A1)}$$

where n is the number of radial nodes $[n=\frac{1}{2}(N-l)]$, and where the Laguerre function is

$$L_n^{l+1}(\alpha r^2)=\sum_{0\le K\le n}(-)^K\binom{n+l+\frac{1}{2}}{n-K}\frac{(\alpha r^2)^K}{K!}.\quad\text{(A2)}$$

The Γ coefficient is then

$$\Gamma_{LM}{}^{\Omega_1\Omega_2\Omega_3\Omega_4}(\alpha,\beta,R)=(-1)^f\left(\frac{2}{\alpha+\beta}\right)^{9/2}(\alpha\beta)^{9/4}\left(\frac{2\alpha}{\alpha+\beta}\right)^{\rho_{\max}+L/2}\times\sqrt{2}(\tfrac{1}{2}!)^{-1/2}(\alpha R^2)^{3/4}\exp(-2\alpha R^2)[2(\alpha+\beta)R^2]^{L/2}\times\sum_\rho\left(\frac{\beta-\alpha}{2\alpha}\right)^{\rho_{\max}-\rho}C_\rho{}^L L_\rho{}^{L+1/2}(2(\alpha+\beta)R^2),\quad\text{(A3)}$$

where $\rho_{\max}=\frac{1}{2}(N_1+N_2+N_3+N_4-L)$ and f is the sum $\sum_i(\,|\,\Omega_i\,|\,-\frac{1}{2})$ carried over orbitals for which Ω_i is negative. $L_\rho{}^{L+1/2}$ is the associated Laguerre polynomial. (Note that for $\beta=\alpha$ the sum over ρ reduces to a single term $\rho=\rho_{\max}$.) The C_ρ coefficients are given by

$$C_\rho{}^L=\frac{\rho!(\frac{1}{2}!)^2}{[L]2^{(2\rho+L)}}\sum_{l_1l_2l_3l_4}\frac{[l_1][l_2][l_3][l_4]B_\rho{}^L(n_il_i)}{[n_1!n_2!n_3!n_4!(n_1+l_1+\frac{1}{2})!(n_2+l_2+\frac{1}{2})!(n_3+l_3+\frac{1}{2})!(n_4+l_4+\frac{1}{2})!]^{1/2}}\times\sum_{\Sigma_1\Sigma_2\Sigma_3\Sigma_4}(-)^{1-\Sigma_1-\Sigma_3+n_1+n_2+n_3+n_4}\delta_{\Sigma_1,-\Sigma_2}\delta_{\Sigma_3,-\Sigma_4}a_{l_1\Lambda_1}a_{l_2\Lambda_2}a_{l_3\Lambda_3}a_{l_4\Lambda_4}D(l_i\Lambda_iL),\quad\text{(A4)}$$

where the $a_{l_i\Lambda_i}$ are the normalized Nilsson wave-function coefficients in Nilsson's original (1955) representation $[Nl\Lambda(\Sigma)\Omega]$; subscripts N and Σ have been suppressed for compactness. The function D is given by

$$D(l_i\Lambda_iL)=\sum_{l_pl_N}(l_1l_2\Lambda_1\Lambda_2\,|\,l_p\Lambda_1+\Lambda_2)\,(l_1l_200\,|\,l_p0)\,(l_3l_4\Lambda_3\Lambda_4\,|\,l_N\Lambda_3+\Lambda_4)\,(l_3l_400\,|\,l_N0)\times(l_pl_N\Lambda_1+\Lambda_2\Lambda_3+\Lambda_4\,|\,LM)\,(l_pl_N00\,|\,L0)\quad\text{(A5)}$$

and

$$B_\rho{}^L(n_i l_i) = (-1)^\rho n_1! n_2! n_3! n_4! \sum_{v_1 v_2 v_3 v_4} \frac{(-1)^{v_1+v_2+v_3+v_4}}{v_1! v_2! v_3! v_4!} \binom{n_1+l_1+\frac{1}{2}}{n_1-v_1} \binom{n_2+l_2+\frac{1}{2}}{n_2-v_2} \binom{n_3+l_3+\frac{1}{2}}{n_3-v_3} \binom{n_4+l_4+\frac{1}{2}}{n_4-v_4}, \quad \text{(A6)}$$

where the summation is restricted by

$$2\rho+L=2(v_1+v_2+v_3+v_4)+l_1+l_2+l_3+l_4. \quad \text{(A7)}$$

The $D(l_i\Lambda_i L)$ is just the integral

$$\int Y_L{}^{\Lambda_1+\Lambda_2+\Lambda_3+\Lambda_4} * Y_{l_1}{}^{\Lambda_1} Y_{l_2}{}^{\Lambda_2} Y_{l_3}{}^{\Lambda_3} Y_{l_4}{}^{\Lambda_4} d\Omega.$$

APPENDIX B: FRÖMAN MATRICES

The elements of the Fröman matrices were calculated from Eq. (12) with the parameter $B=0.9$ as explained earlier. Numerical integration was performed on an IBM 7094 computer using Gaussian quadrature with 100 equal intervals in θ, taking two points in each interval. The values for the spherical harmonics were calculated using an adaptation of the IBM SHARE routine JP ASLF which calculates the associated Legendre polynomials from recursion relations. All matrices in Table IX require a total of about a minute to calculate.

The accuracy of the program was checked in two ways. First, the parameter B was set to zero and, when rounded to five decimal places, the calculations gave the unit matrix as required by the orthonormality property of the spherical harmonics. Secondly, the calculations were repeated with $B=0.9$, but with 200 intervals instead of 100. The differences in the matrix elements were never larger than two units in the sixth decimal place. We may thus state that accumulated roundoff errors will not affect the four decimal places given in Table IX.